# AIRBORNE REMOTE SENSING
# THERMAL INFRARED & LIDAR

## CHRISTMAS VALLEY, OREGON MILITARY, PAULINA MARSH, & BAKER PASS • OREGON

Delivery 2 V.2 07/13/2012

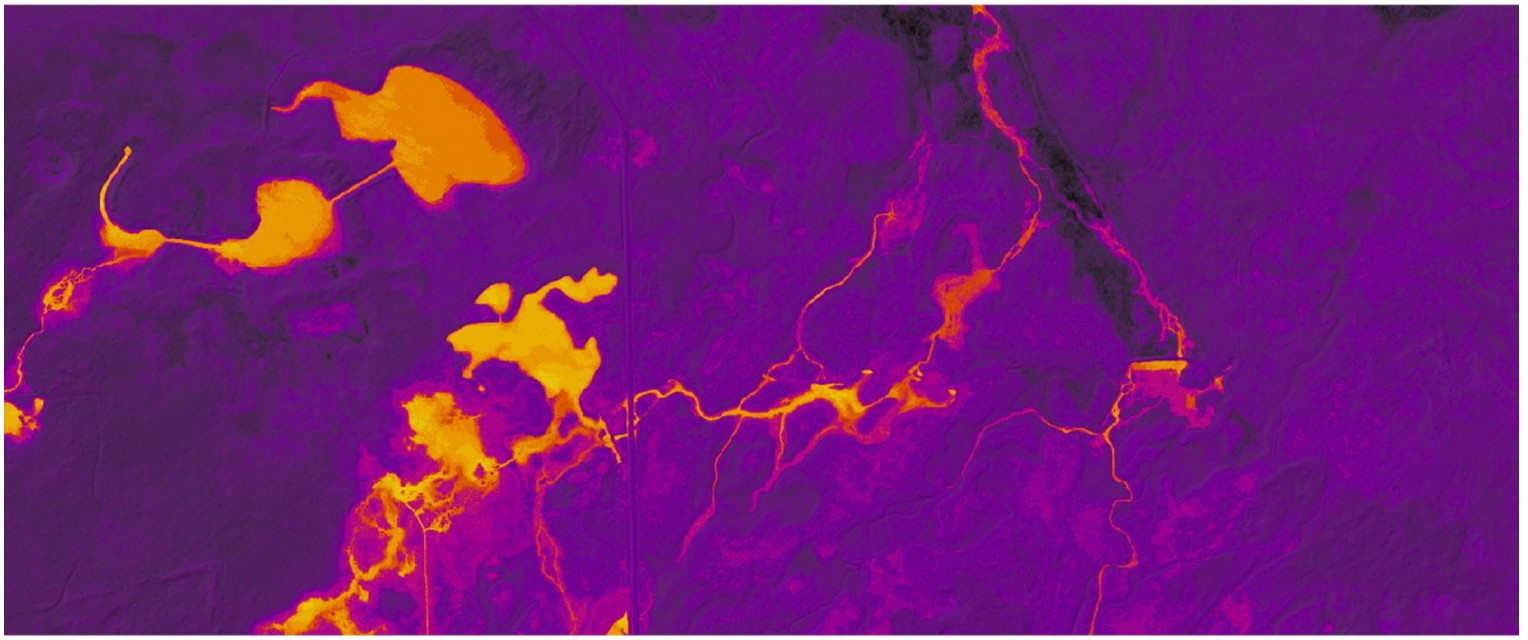

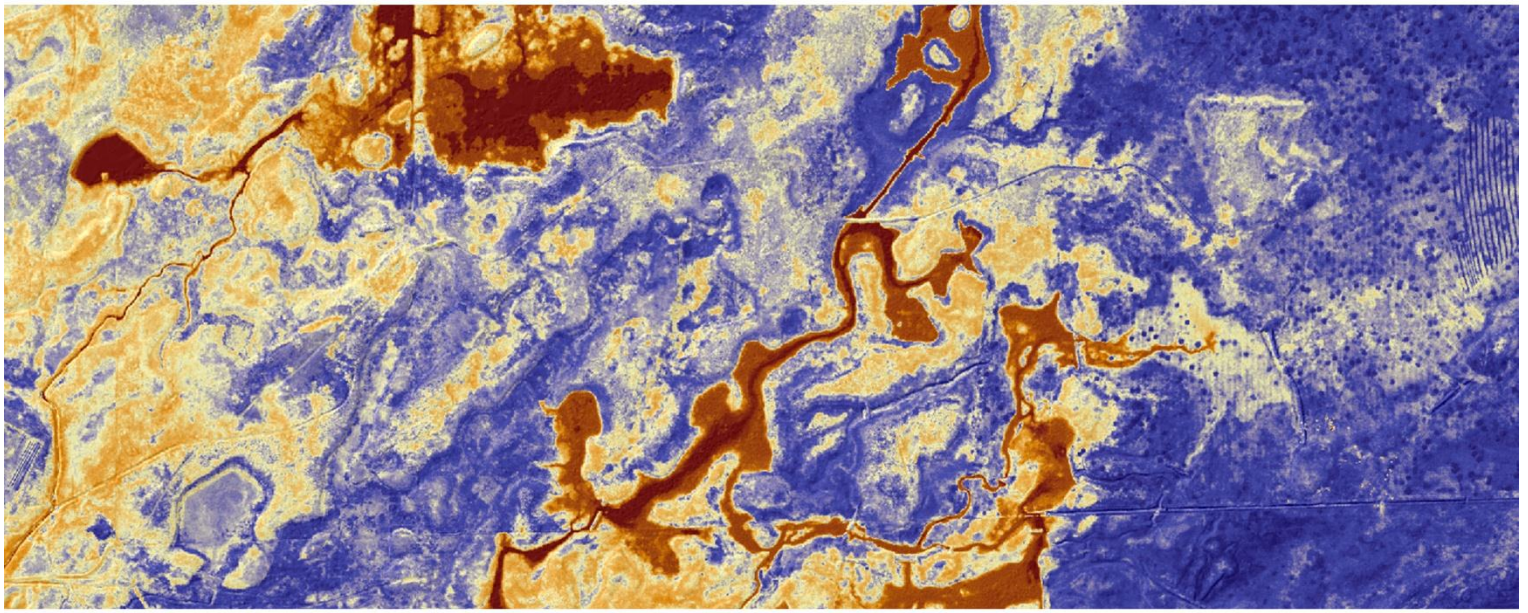


**OREGON DEPARTMENT OF GEOLOGY AND MINERAL INDUSTRIES**

**CLARK NIEWENDORP** - 800 NE Oregon St., #28, Suite 965 - Portland, OR 97232

**WATERSHED SCIENCES** • 517 SW 2nd Street, Suite 400 - Corvallis, OR 97333

# DEPARTMENT OF GEOLOGY & MINERAL INDUSTRIES
## AIRBORNE REMOTE SENSING: THERMAL INFRARED & LIDAR

### DELIVERY 2 V.2: CHRISTMAS VALLEY, OR MILITARY, PAULINA MARSH, & BAKER PASS OREGON

TABLE OF CONTENTS

# 1. Overview

Watershed Sciences, Inc. (WSI) collected airborne Thermal Infrared (TIR) imagery and Light Detection and Ranging (LiDAR) data for the Department of Geology and Mineral Industries (DOGAMI) in Malheur, Harney, and Lake Counties during March and April 2012. This is the final delivery encompassing the four remaining study areas of the DOGAMI TIR and LiDAR survey. The requested acreage for Christmas Valley (13,041 acres), Oregon Military (9,701 acres), Paulina Marsh (56,287 acres), and Baker Pass (44,846 acres) study areas were expanded to include a 100m buffer to ensure complete coverage around survey area boundaries. This expansion results in a total of 13,809 acres, 10,344 acres, 57,768 acres, and 46,194 acres of delivered TIR and LiDAR data, respectively (Figure 1). The TIR imagery provides an accurate data set for detecting and identifying surface expression of geothermal activity. LiDAR data was co-acquired with the TIR imagery and provides highly detailed topographic data for recognizing landforms associated with detected thermal features.

Airborne TIR remote sensing has proven to be an effective method for mapping spatial temperature patterns on terrestrial surfaces. The TIR imagery illustrates the location and thermal influence of point sources, terrestrial springs, and evidence of geothermal activity.

***Figure 1**. The Department of Geology and Mineral Industries TIR and LiDAR remote sensing survey consisted of the previously delivered Summer Lake study area and the Christmas Valley, Oregon Military, Paulina Marsh, and Baker Pass study areas present in this delivery*

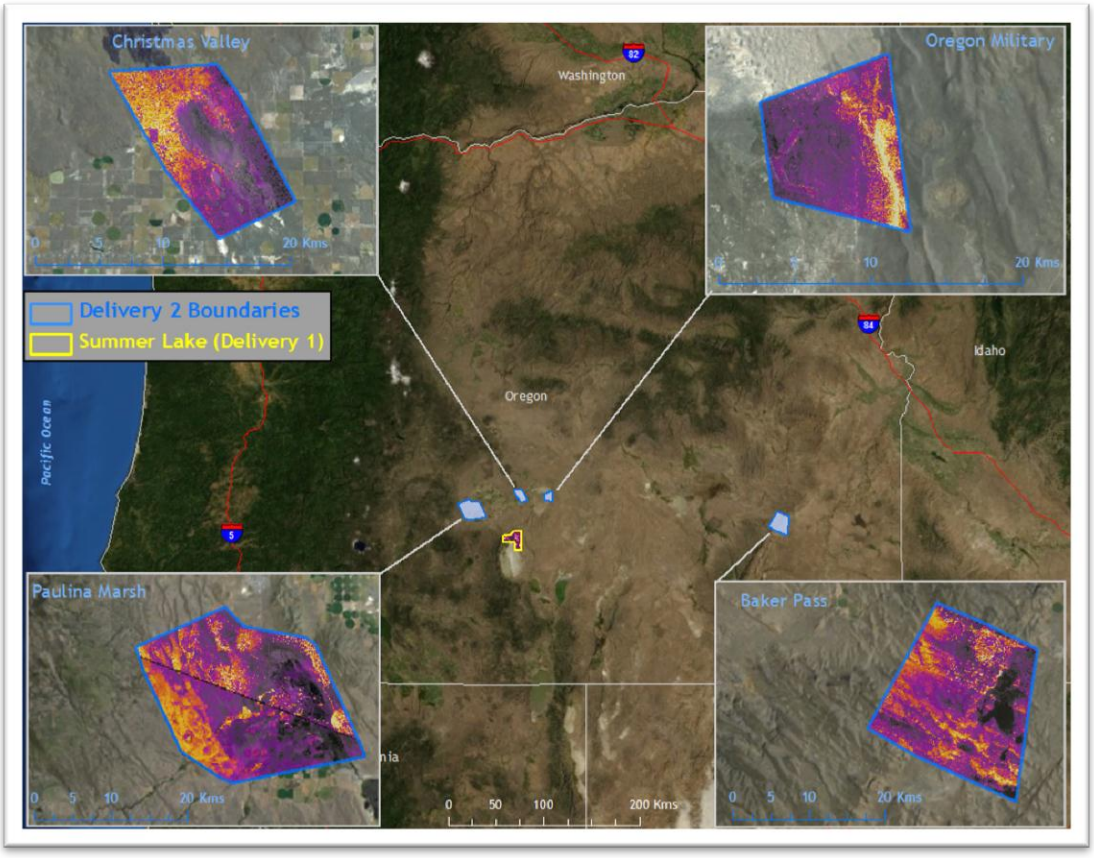

# 2. Thermal Infrared (TIR) Imagery

## 2.1 TIR Acquisition

### *2.1.1 Airborne Instrumentation*

TIR images were collected with a FLIR Systems SC6000 sensor (8-9.2μm) mounted in the Cessna Caravan. The SC6000 has a 640x512 QWIP detector array capable of collecting 14-bit digital frames directly from the sensor to an on-board computer. The SC6000 is a calibrated radiometer with a NETD of 0.05°C, internal non-uniformity correction and drift compensation. Images are initially collected in a binary data format representing the measured, emitted radiance in the scene. The TIR sensor has a 50mm lens resulting in a total horizontal field-of-view of 18°. General specifications of the thermal infrared sensor are listed in Table 1.

Thermal infrared images were recorded directly from the sensor to an on-board computer as raw counts, which were then converted to radiant temperatures (°K * 10) based on the calibration coefficients of the sensor and the recorded environmental conditions. The individual images were referenced using an IRIG-B time-code generated from an onboard GPS. The aircraft position and attitude (pitch, roll, and yaw) were precisely recorded using an on board GPS/IMU. The image frames were linked to the GPS/IMU data during the post processing.

***Table 1**. Summary of TIR sensor specifications*

| | |
|---|---|
| **Sensor:** | FLIR System SC6000 (LWIR) |
| **Wavelength:** | 8-9.2 μm |
| **Noise Equivalent Temperature Differences (NETD):** | 0.035°C |
| **Pixel Array:** | 640 (H) x 512 (V) |
| **Encoding Level:** | 14 bit |
| **Horizontal Field-of-View:** | 18.0° |


***Figure 2**. Pictures above are WSI's FLIR SC6000 integrated with a Leica ALS50-Phase II LiDAR System installed in one of WSI's Cessana Caravans. The SC6000 utilizes the same GPS/IMU system as the LiDAR system for direct computation of image external orientation*

### *2.1.2 Ground Control*

#### *2.1.2.1 Static Survey Data*

Ground survey data were collected to enable the geo-spatial correction of the aircraft positional coordinate data collected throughout the flight. During the flight, 1 Hz static ground surveys were conducted over monuments using a Trimble GNSS model R7 Zephyr Geodetic Model 2 (OPUS ID: TRM57971.00) antenna with ground plane and a Trimble R8 GNSS Model 2 (OPUS ID: TRM_R8_GNSS) receiver were deployed for all static control (Table 2). All GPS measurements were made with dual frequency L1-L2 receivers with carrier-phase correction.


***Figure 3**. Image of a control monument for the Christmas Valley study area*

WSI established 8 new monuments to total 10 for the entire DOGAMI TIR project. The monumentation was done with 5/8" x 30" rebar topped with a metal cap stamped with "Watershed Sciences, Inc," the monument ID, and the year of establishment.

***Table 2**. Control Monuments for each Delivery 2 survey area*

***Summer Lake***

| Base Station ID | Datum: NAD83 (CORS96) | | GRS80 |
|---|---|---|---|
| | Latitude | Longitude | Ellipsoid Z (meters) |
| DOGAMI 7 | 43°00' 19.91633" | 120°43' 53.26249" | 1272.667 |
| DOGAMI 8 | 42°57' 54.05452" | 120° 38' 56.27157" | 1276.375 |

***Christmas Valley***

| Base Station ID | Datum: NAD83 (CORS96) | | GRS80 |
|---|---|---|---|
| | Latitude | Longitude | Ellipsoid Z (meters) |
| DOGAMI 3 | 43°19' 28.70911" | 120°36' 58.79413" | 1312.071 |
| DOGAMI 4 | 43°15' 59.57374" | 120°34' 42.85245" | 1311.247 |

***Oregon Military***

| Base Station ID | Datum: NAD83 (CORS96) | | GRS80 |
|---|---|---|---|
| | Latitude | Longitude | Ellipsoid Z (meters) |
| DOGAMI 5 | 43°18' 19.35923" | 120°20' 09.30771" | 1346.676 |
| DOGAMI 6 | 43°15' 48.39494" | 120°20' 09.01841" | 1316.367 |

***Paulina Marsh***

| Base Station ID | Datum: NAD83 (CORS96) | | GRS80 |
|---|---|---|---|
| | Latitude | Longitude | Ellipsoid Z (meters) |

| | | | |
|---|---|---|---|
| DOGAMI 1 | 43°13’ 01.27405” | 121°08’ 17.90558” | 1366.824 |
| DOGAMI 2 | 43°08’ 47.83455” | 121° 02’ 08.04853” | 1320.730 |

***Baker Pass***

| Base Station ID | Datum: NAD83 (CORS96) | | GRS80 |
|---|---|---|---|
| | Latitude | Longitude | Ellipsoid Z (meters) |
| DOGAMI 9 | 43°08’ 00.52599” | 118°06’ 54.34028” | 1255.008 |
| DOGAMI 10 | 43°04’ 29.21270” | 118°11’ 26.78361” | 1358.118 |

### *2.1.2.2 Air Targets*

Air targets were distributed in the study area in order to quantify the spatial accuracy of geo-rectified TIR imagery. Air targets consisted of space blankets and small, catalytic portable heaters (Figure 7). The target locations were surveyed using real time kinematic (RTK) techniques. The distribution of air targets in each survey area are illustrated with their associated image frame index in Figures 3-6.

***Figure 3****. Air target and image frame locations for the Christmas Valley study area*

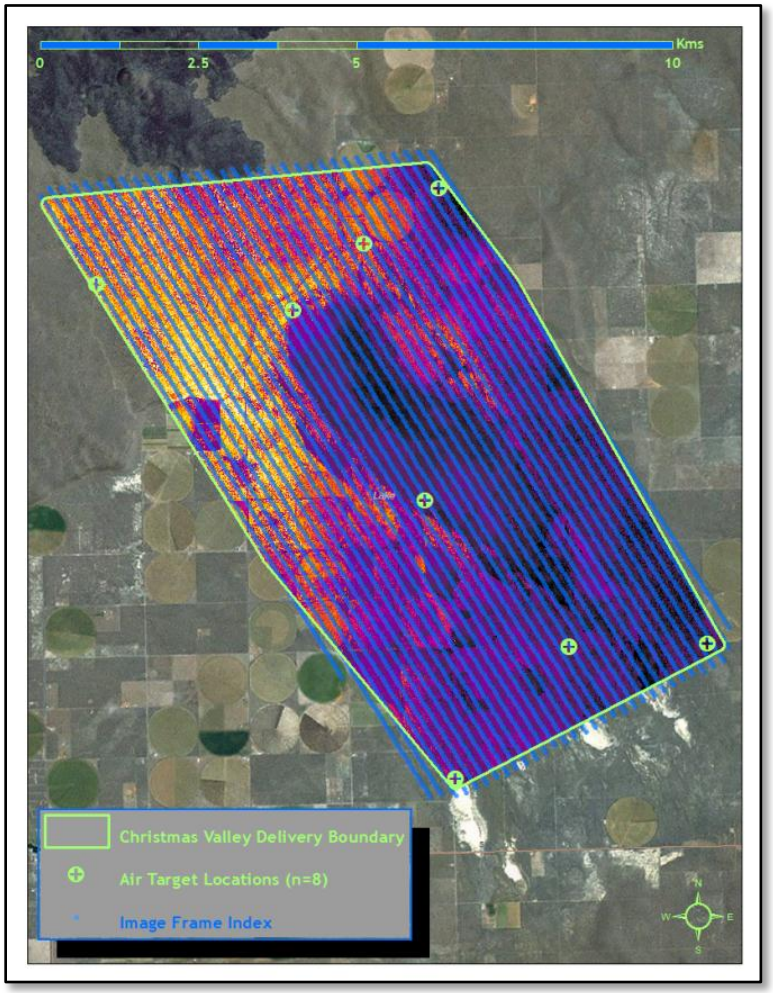

***Figure 4**. Air target and image frame locations for the Oregon Military study area*

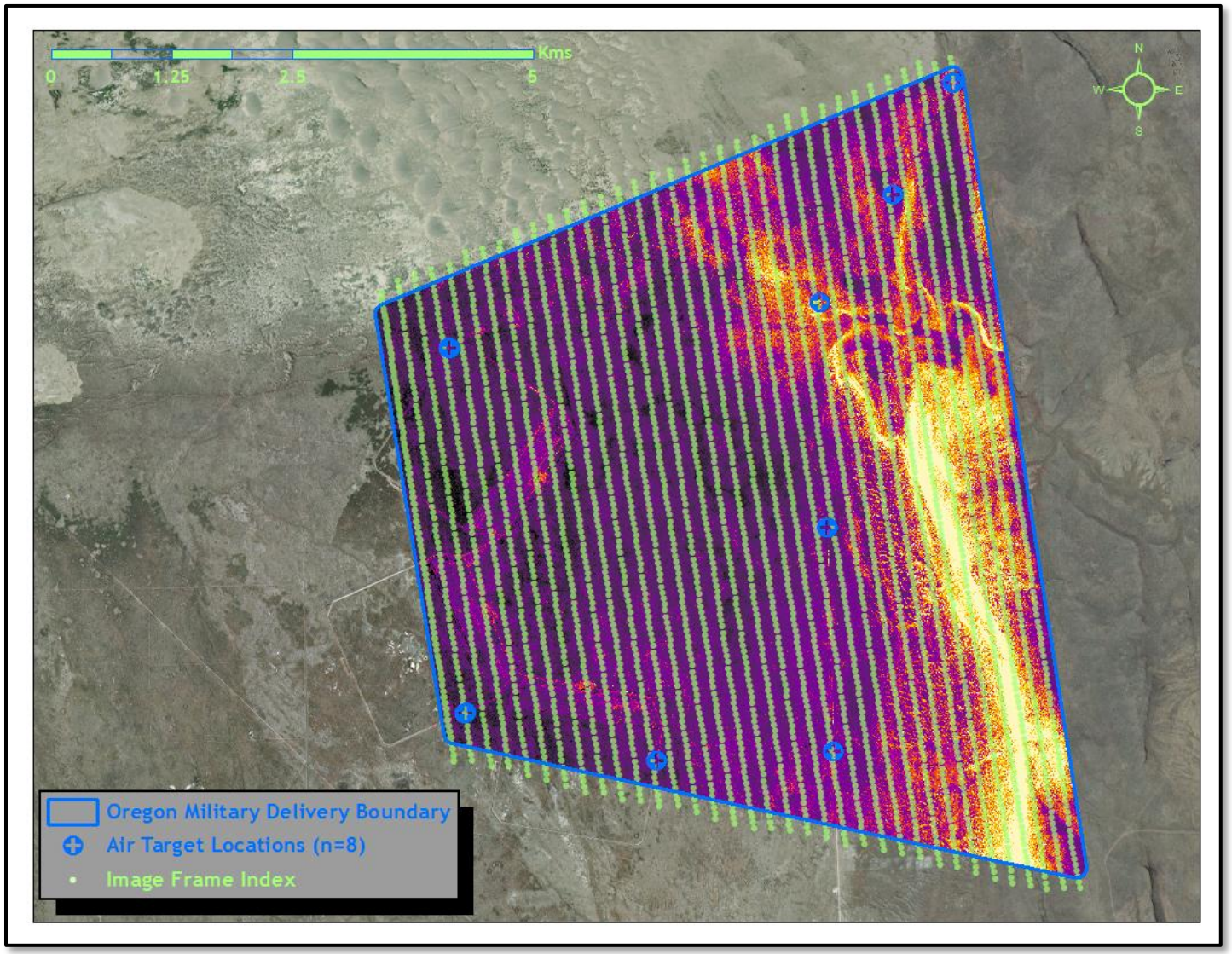

***Figure 5**. Air target locations deployed for the Paulina Marsh study area*

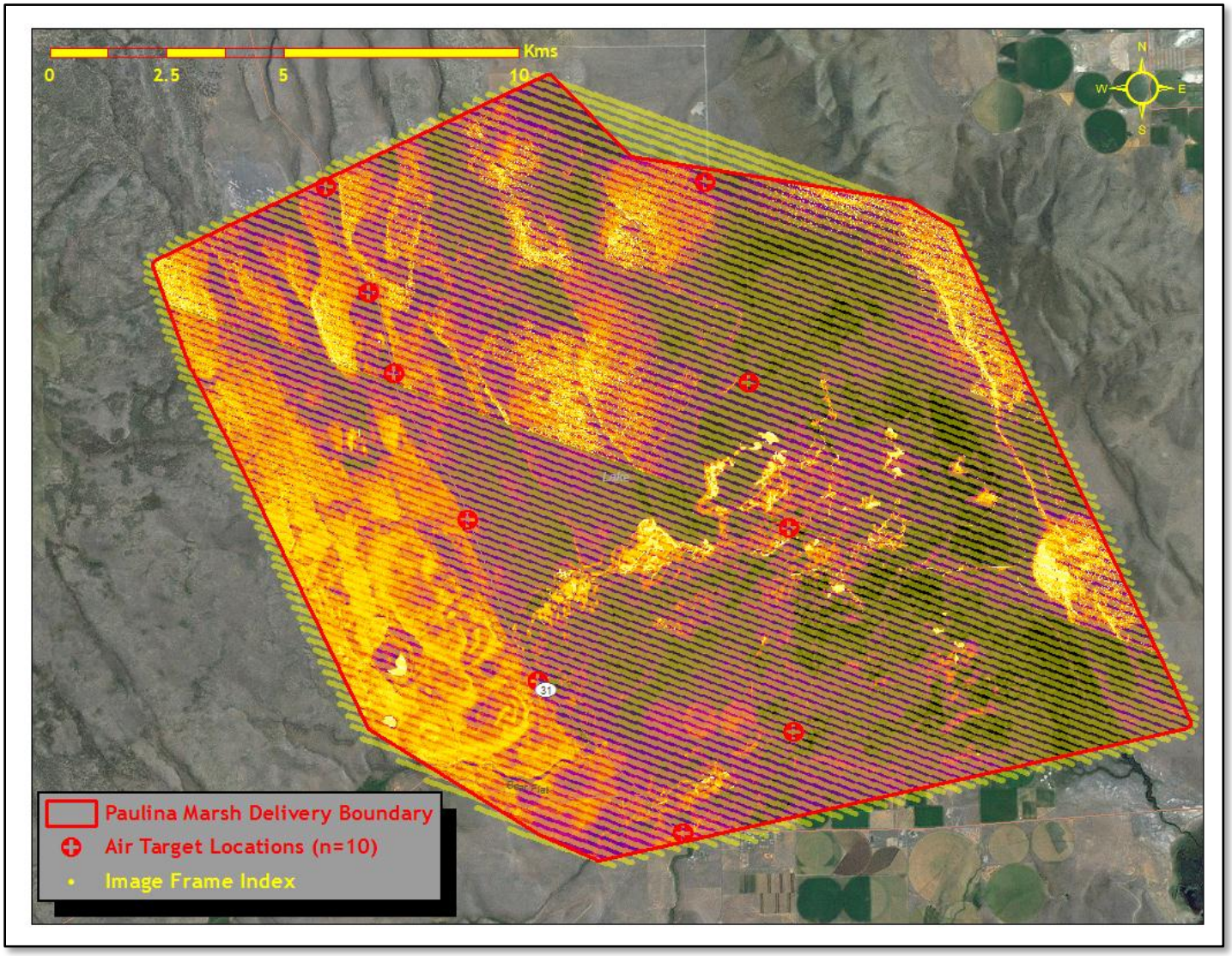

***Figure 6**. Air target locations deployed for the Baker Pass study area*

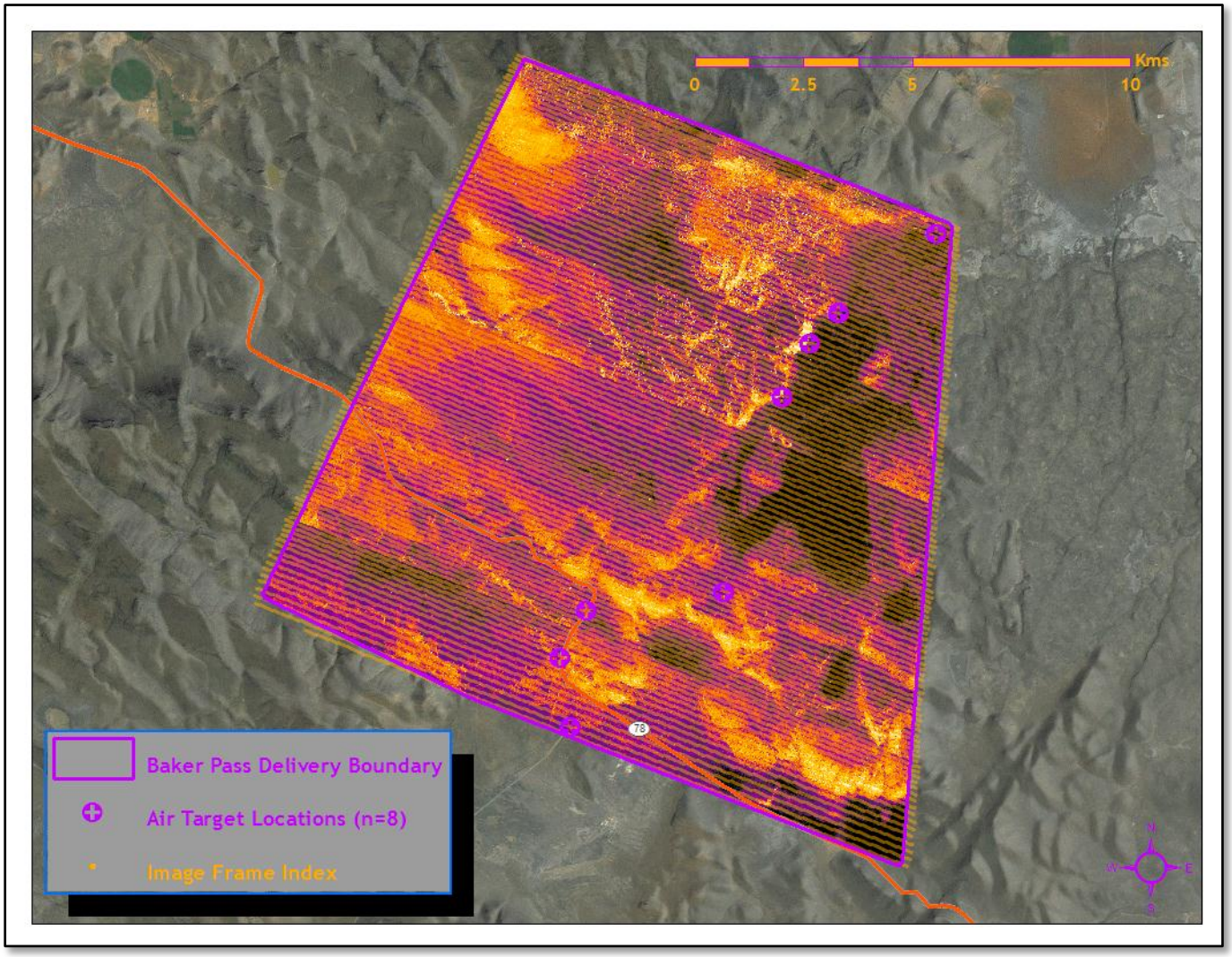

***Figure 7****. GPS base station set up with "space" blanket target set up near the control monument. The space blanket has a very low emissivity compared to the surrounding terrain and is detectable in the TIR imagery. The blankets were paired with small, catalytic heaters to quantify the accuracy of the TIR mosaic*

### *2.1.3 Acquisition Summary*

The aircraft was flown in parallel flight lines in order to capture the entire requested area. The flight lines were designed for an image side-lap of 40% while the TIR sensor was set to acquire images at a rate of 1 image every second resulting in an image overlap of approximately 60%. The TIR data acquisition was conducted at a flight altitude of 1100 meters above ground level (AGL) resulting in a native pixel resolution of 0.5m. A summary of acquisition parameters and flight times can be seen in Table 3.

Flight planning was developed to capture the greatest possible temperature difference between geothermal sources and ambient temperatures of the surrounding landscape. Acquisition began shortly after midnight and was completed just before dawn (*Environmental information reported below (Table 3) from the "Weather Underground" website as recorded in Bend and Burns, OR (http://www.wunderground.com/)*). These weather stations were selected specifically for their detailed records as regular as every 10-20 minutes and their proximity to the project area (historic weather records for the closest weather stations in Paulina, Fort Rock, and Rome OR are not as in depth or extensive). Also due to the size of the Paulina Marsh and Baker Pass project areas, multiple days were needed to acquire the entire project area within optimal hours. Subsequently, those two project areas are being delivered by date of acquisition (Paulina Marsh 03/08 & 03/09 2012, and Baker Pass 04/06-04/08 2012).

***Table 3**. Environmental and flight information for the co-acquisition of each Delivery 2 study area*

| | Acquisition | | | Temperature (°F) | | | | |
|---|---|---|---|---|---|---|---|---|
| | Date | Time (24hrs) | Sunrise (24hrs) | Begin | End | Frames | (AGL) | Pixel Size |
| Christmas Valley | *3/3/2012* | *0115 - 0515* | *0634* | *37* | *37* | 5,693 | ***1100*** | ***0.5 meters*** |
| Oregon Military | *3/5/2012* | *0100 - 0430* | *0631* | *44* | *43* | 3,966 | ***1100*** | ***0.5 meters*** |
| Paulina Marsh | *3/8/2012* | *0005 - 0610* | *0627* | *28* | *32* | 12,395 | ***1100*** | ***0.5 meters*** |
| | *3/9/2012* | *0010 - 0550* | *0625* | *45* | *37* | 11,576 | | |
| Baker Pass | *4/6/2012* | *0000 - 0300* | *0723* | *27* | *24* | 4,179 | ***1100*** | ***0.5 meters*** |
| | *4/7/2012* | *2345 - 0600* | *0721* | *19* | *21* | 10,299 | | |
| | *4/8/2012* | *2340 - 0620* | *0719* | *37* | *29* | 9,549 | | |

### *2.1.4 Temperature Calibration*

WSI deployed eight data loggers (Onset Hobo-Pros) during the time frame of the flight for calibrating and verifying the thermal accuracy of the TIR imagery for all the project areas. The WSI Hobo Pro data loggers were set to record temperatures at 10 minute intervals and suspended in the water throughout the study area. Six of the data loggers were deployed in the Summer Lake project area on March 3rd, 2012, and retrieved after the Christmas Valley study area had been acquired on March 4th, 2012. The other two loggers were deployed in the Paulina Marsh project area on March 8th, and retrieved on March 9th, 2012. All data logger locations and their respective serial number can be found in Figure 8.

***Figure 8**. Hobo Data Logger locations and serial numbers used for the DOGAMI TIR project*

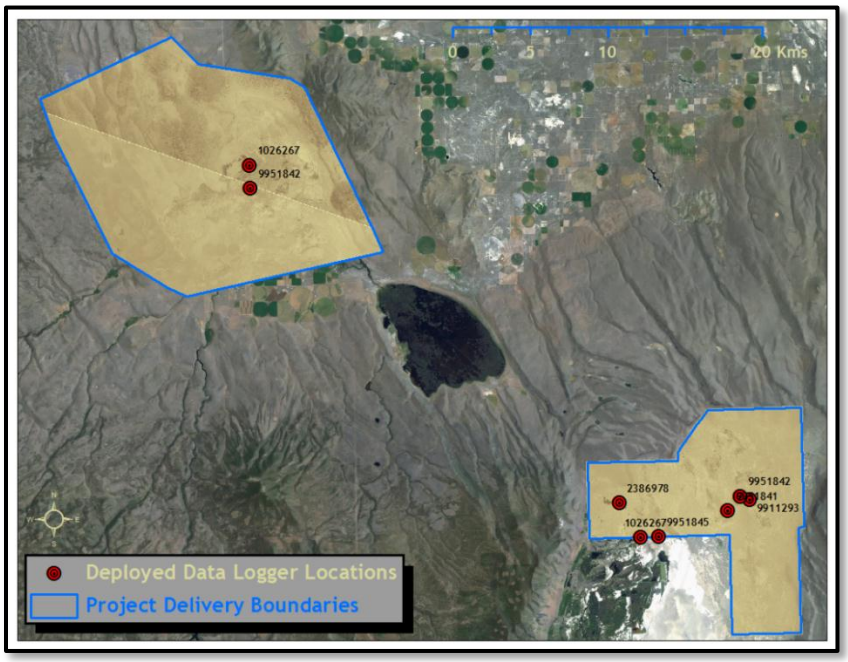

## *2.2 Thermal Image Characteristics*

### *2.2.1 Surface Temperatures*

The TIR imagery was flown pre-dawn to ensure the terrestrial temperatures would be cool relative to any hot springs. The objective was to achieve the maximum thermal contrast between terrestrial features and surface springs or geothermal anomalies. In the pre-dawn hours, hot springs and other surfacial expressions of geothermal activity should reflect higher temperatures than the surrounding features within the thermal infrared scene. Since water is essentially opaque to TIR wavelengths, the sensor only measures water surface temperatures. The imagery will highlight surfacial expression, such as thermal plumes for surface springs or near surface activity; however, detection of sub-surface discharge will depend on depth and vertical mixing rates at that location.

### *2.2.2 Expected Accuracy*

Thermal infrared radiation received at the sensor is a combination of energy emitted from the earth's surface, reflected from the earth's surface, and absorbed and re-radiated by the intervening atmosphere. Water is a better emitter of TIR radiation and has relatively low reflectivity (~ 4 to 6%). Surface and atmospheric conditions (path length transmission) can result in some variability in the resulting radiant temperature measurements. In general, radiant temperatures may show frame-to-frame thermal variability of up to 0.5°C

### *2.2.3 Image Uniformity*

The TIR sensor deployed for this study used a focal plane array of detectors to sample incoming radiation. A challenge when using this technology is to achieve uniformity across the detector array. The sensor has a correction scheme which reduces non-uniformity across the image frame. However, differences in temperature can be observed near the edge of the image frame. During processing, we trim the image frames by at least 10% in order to minimize the impact of non-uniformity near the frame edge. Interpretation of the TIR images should consider the inherent thermal variability within the image and use caution when interpreting thermal differences less than ~0.5°C unless they are associated with a distinct thermal discharge.

### *2.2.4 Temperatures and Color Maps*

The TIR images collected during this survey consist of a single band. As a result, visual representation of the imagery *(in a report or GIS environment*) requires the application of a color map or legend for the pixel values. The selection of a color map should highlight features most relevant to the analysis (i.e. *identify geothermal activity within the project area*). For example, a continuous, gradient style color map that incorporates all temperatures in the image frame will provide a smoother transition in colors throughout the entire image, but may not highlight changes of temperature at a localized scale and fail to identify source sites. Conversely, a color map that focuses too narrowly cannot be applied to the entire project area and will washout relevant features (Figure 6).

***Figure 9**. Color ramp comparison of a ground spring section of the Paulina Marsh study area (bottom right corner is 2011 NAIP of Lake County, the remaining images are all thermal mosaics with different color ramps to demonstrate contrast variability)*

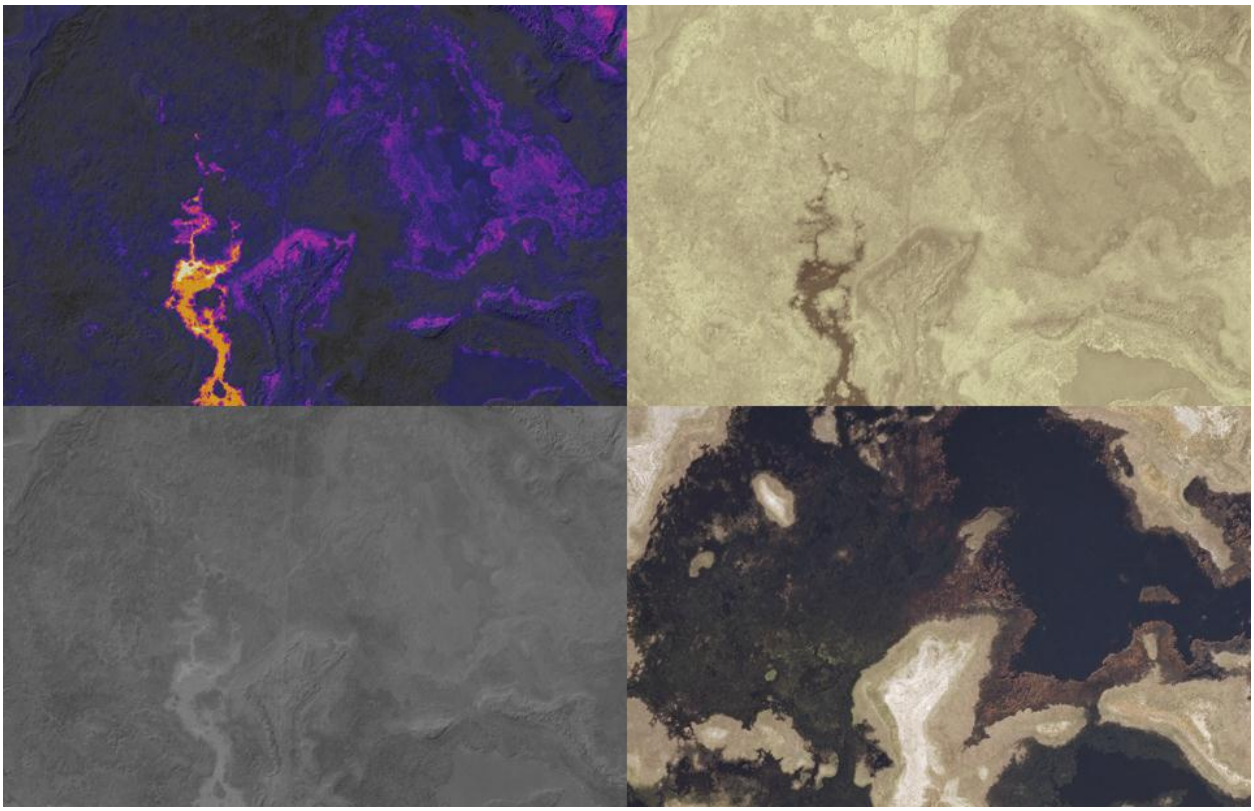

## 2.3 Data Processing

### *2.3.1 Sensor Calibration*

The response characteristics of the TIR sensor are measured in a laboratory environment. The response curves relate the raw digital numbers recorded by the sensor to emitted radiance from a black body. The raw TIR images collected during the survey initially contain digital numbers which are then converted to radiant temperatures based on the factory calibration.

The calculated radiant temperatures are adjusted based on the kinetic temperatures recorded at each ground truth location. This adjustment is performed to correct for path length attenuation and the emissivity of natural water. The data are assessed at the time the image is acquired, with radiant values representing the median of ten points sampled from the image at the data logger location.

### *2.3.2 Ortho-Rectification of Imagery*

Light Detection and Ranging (LiDAR) data were collected simultaneously with the TIR flight (*LiDAR methods and results are included in Section 3 of this report*). The following data layers were derived from the LiDAR data and used in TIR image processing:

- 1 meter pixel resolution bare-earth digital surface model (DEM): Used for ortho-rectification of the TIR imagery.
- 0. 5 meter pixel resolution LiDAR intensity image: Used for the QA/QC of the final TIR mosaic and assist in the measurement of ground targets during accuracy assessment.

### *2.3.3 Kinematic GPS Data*

While surveying, the aircraft collects kinematic GPS data and the onboard inertial measurement unit (IMU) collects aircraft attitude data. The positional datasets are referenced to static ground GPS that are set up prior to the TIR survey flight. IPAS-TC is used to process the kinematic corrections for the aircraft. The static and kinematic GPS data are then post-processed after the survey to obtain accurate GPS solution and aircraft positions during times of the survey. IPAS-TC 3.1 is used to develop a trajectory file that includes corrected aircraft position and attitude information. The trajectory data for the entire flight survey session is incorporated into a final smoothed best estimate of trajectory (SBET) file that contains accurate and continuous aircraft positions and attitudes. An exterior orientation file is derived from the SBET file by calculating GPS positions and orientation angles of the sensor at each image capture time and applying lever arm and misalignment angle offsets.

### *2.3.4 Image Rectification Workflow and Applications*

1. Monument static GPS data are processed with aircraft GPS data to resolve kinematic corrections.

   **Software:** IPAS-TC
2. Aircraft attitude data are incorporated with the post processed aircraft kinematic GPS data.

   **Software:** IPAS-TC
3. For each camera exposure event, an exterior orientation is calculated for the perspective center (image center point position X,Y,Z) and orientation angles of the image (omega, phi, kappa), which describe the relationship between the camera mapping frame and the ground.

   **Software:** IPAS-CO
4. Integrated photogrammetric processing of the TIR images. Interior orientation of the FLIR sensor were derived and input into LPS. LPS applies the exterior orientation to images. Ortho-rectification resampling was performed through LPS using the LiDAR derived bare-earth model for elevation values. Images were resampled (nearest neighbor technique) at a ground sample distance of 0.5 meters.

   **Software:** LPS
5. Automatic seam generation and mosaic creation from thermal-images. No adjustments were made to color or contrast so temperature information was preserved.

   **Software:** OrthoVista

### *2.3.5 Spatial Accuracy Assessment*

For each study area in this delivery air targets were deployed and survey coordinates were taken on each target location (Christmas Valley (n = 16), Oregon Military (n= 16), Paulina Marsh (n=20), and Baker Pass (n=16)). Thermal "space" blankets and Coleman Sport catalytic heaters were used as the air target pairs at each site, Figure 10 shows an example of an air target pair, one blanket & one burner). RTK was recorded for spatial reference at all corners of each thermal blanket and at every heater location. Final TIR mosaics were evaluated for spatial accuracy based on the location of these reference points on the imagery. The accuracy is expressed as root mean square error (RMSE) and was calculated by measuring the difference between air target RTK and the locations on TIR imagery. Figure 10 displays a Summer Lake (previous delivery) air target location where both types of targets were set up, and demonstrates the accuracy of the imagery by comparing location of the target(s) with the RTK.

***Figure 10**. Air target location used for spatial accuracy assessment. The air target RTK locations are represented by the turquoise dots (blanket on the left and the single point over the heater is on the right) and a control monument is represented by the yellow triangle*

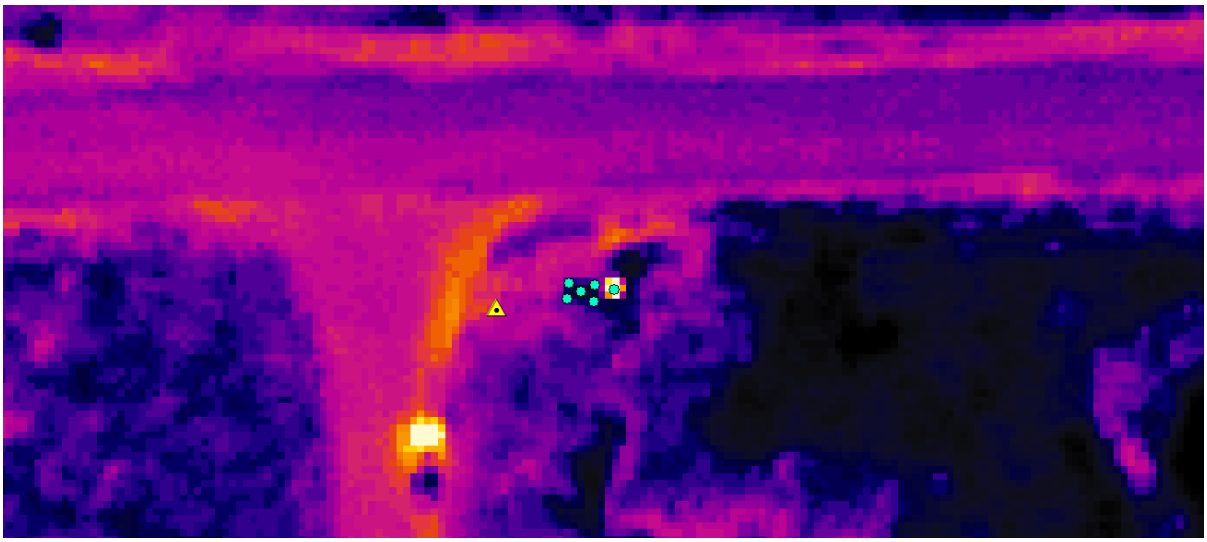

## 2.4 Study Area Results

The objective of this project was to identify geothermal activity in the Christmas Valley, Oregon Military, Paulina Marsh, and Baker Pass study areas. Acquisition flights were conducted in pre-dawn hours to maximize the thermal contrast between the hot springs, seeps, and features with possible geothermal signatures from their surrounding cooler terrestrial environment. With acquisition early in the morning, residual thermal loading from the sun was minimized allowing the highest probability of detection for warmer features that would indicate near surface geothermal activity. Given the seasonality and time of acquisition, geothermal influenced land and water forms should be easily identifiable in the imagery.

As stated earlier, Paulina Marsh and Baker Pass project areas took several days to fully acquire the entire survey area within the most optimal conditions. The days of acquisition happened to align with a warming trend in each instance. For example, 46 ºF was the daily high temperature on March 7th, 2012. After the first acquisition flight of Paulina Marsh on March 8th, 2012 the high temperature was twenty degrees warmer, at 66 ºF. Although not as extreme, the daily high temperature on April 6th, 2012 (42 ºF on the first day of acquisition of Baker Pass) was 15 degrees cooler than the daily high the following day (57 ºF on April 7th). The temperatures at time of acquisition were very similar, but the increase in daily high temperatures the day before very well explain temperature differences found in adjacent images along seams due to thermal loading (Figure 11). This creates nonhomogeneous seams between dates of acquisition, but these differences were kept to retain the authenticity of the data.

WSI found less surface expression of geothermal activity throughout these study areas than in the previous delivery of Summer Lake. There were a few landforms and geothermal expressions found in the imagery. Paulina Marsh and the surrounding surface springs highlight the findings from these data. Not surprising, the two study areas with extensive surface water demonstrate the most easily identifiable surface expression. There were a few isolated surface springs and areas of thermal intrigue in Baker Pass and Christmas Valley. The LiDAR was much more informative in each instance. In the Christmas Valley study area, several lineaments were identified trending in a general north northeast to south southwest direction (Figure 18). These landforms run in a parallel trajectory to the well-known Crack in the Ground which lies in the extreme northwestern corner of the study area.

Several thermal artifacts were identified in the original Delivery 2 shipment for Baker Pass. These offsets were significant enough in adjacent frames of the southeastern portion of the project area for WSI to recalibrate these images. The images made up a small portion of the entire project area, and of the 24, 027 thermal frames for Baker Pass, only 290 (1.21%) were affected and recalibrated (0.42% of the total project frames). Those recalibrated rectified frames and mosaics were redelivered with the Task 5 close out delivery.

***Figure 11****. The images are temperature profiles taken from every hour during the acquisition of each of the Delivery 2 study areas for the DOGMAI TIR project (Hours of acquisition are in contrasting colors and highlighted by the names and arrows identifiers, The first two profiles are temperatures recorded from the Bend Airport and the bottom profile is from Burns, Oregon)*

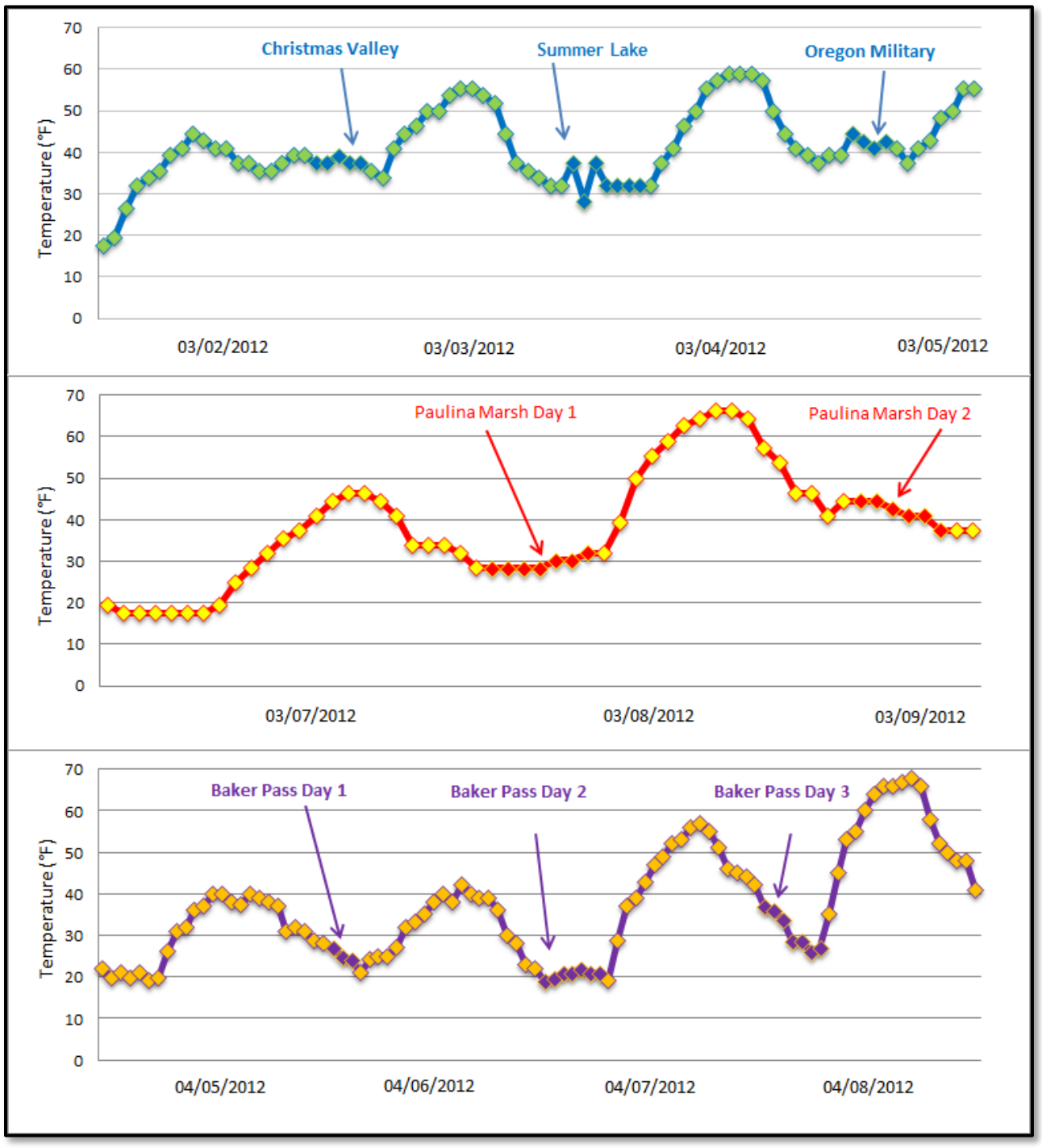

### *2.4.1 Spatial Accuracy for Thermal Imagery*

***Table 4**. Spatial Accuracy Assessment for the Delivery 2 final mosaics of the DOGAMI TIR project*

| | Mean | Standard Deviation (*1 Sigma*) | Root Mean Square Error (*RMSE*) |
|---|---|---|---|
| Summer Lake TIR | 0.12 m | 0.49 m | 0.50 m |
| **Christmas Valley TIR** | 0.08 m | 0.55 m | 0.54 m |
| **Oregon Military TIR** | 0.15 m | 0.32 m | 0.35 m |
| **Paulina Marsh TIR** | 0.03 m | 0.36 m | 0.35 m |
| **Baker Pass TIR** | 0.09 m | 0.32 m | 0.32 m |

***Figure 12**. Accuracy residuals from comparing RTK of air targets with locations on final thermal mosaics for the previously delivered Summer Lake study area (units representing accuracy on both axes are in meters)*

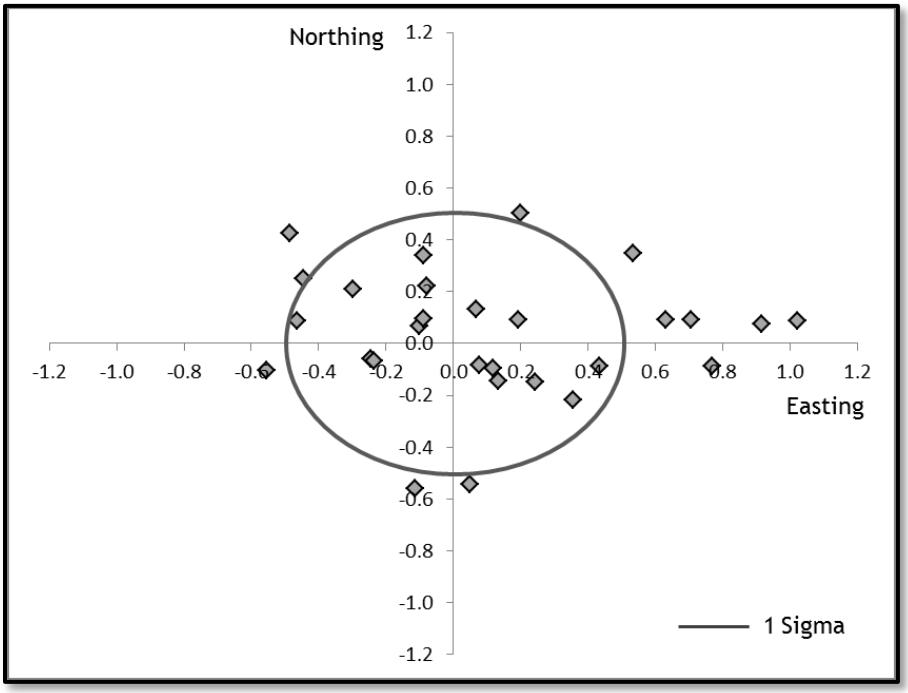

***Figure 12**. Accuracy residuals from comparing RTK of air targets with locations on final thermal mosaics for the Christmas Valley study area (units representing accuracy on both axes are in meters)*

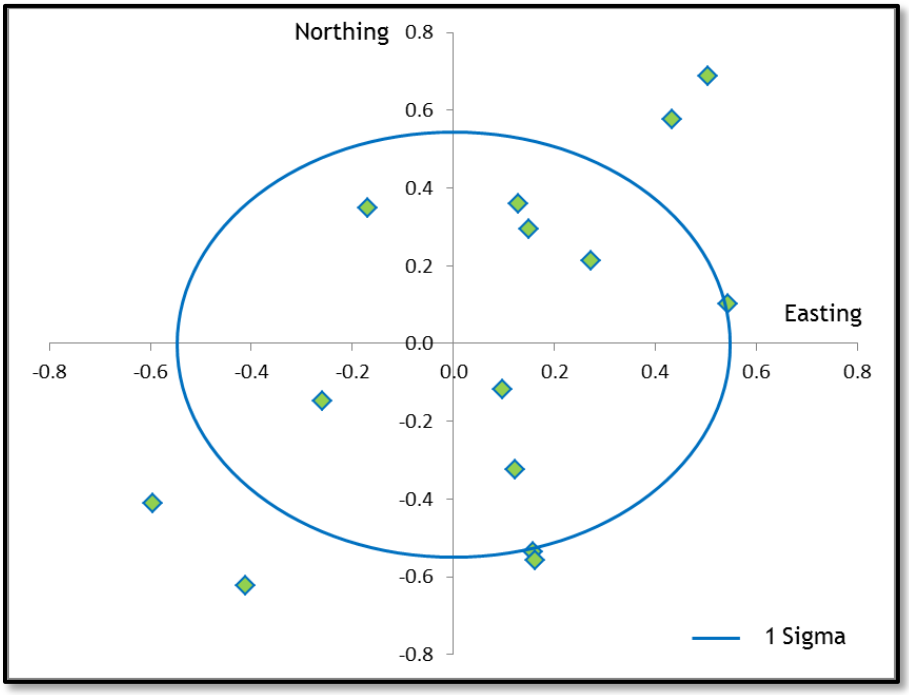


***Figure 13**. Accuracy residuals from comparing RTK of air targets with locations on final thermal mosaics for the Oregon Military study area (units representing accuracy on both axes are in meters)*

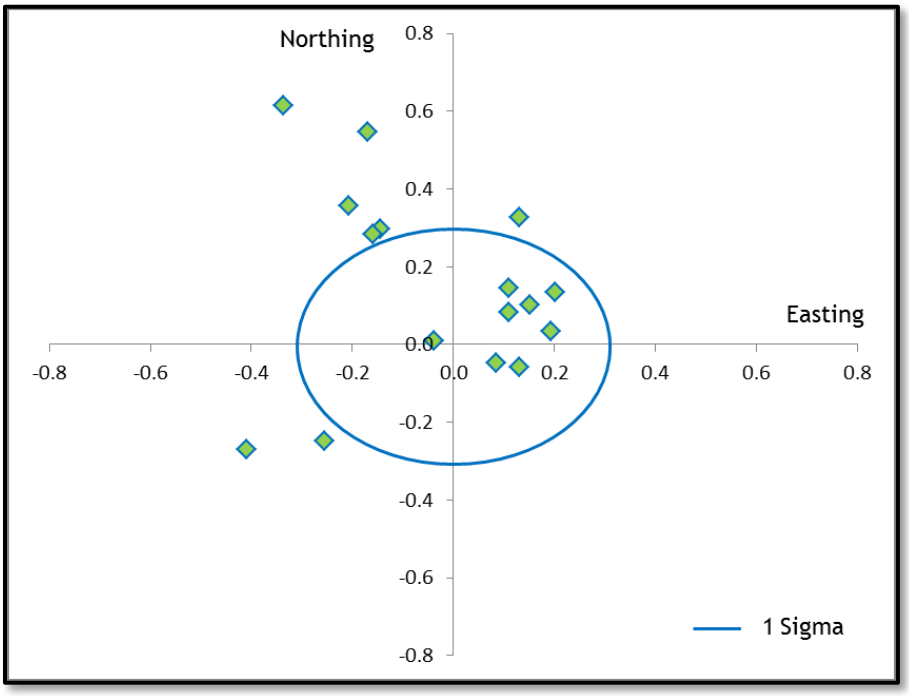

***Figure 14**. Accuracy residuals from comparing RTK of air targets with locations on final thermal mosaics for the Paulina Marsh study area (units representing accuracy on both axes are in meters)*

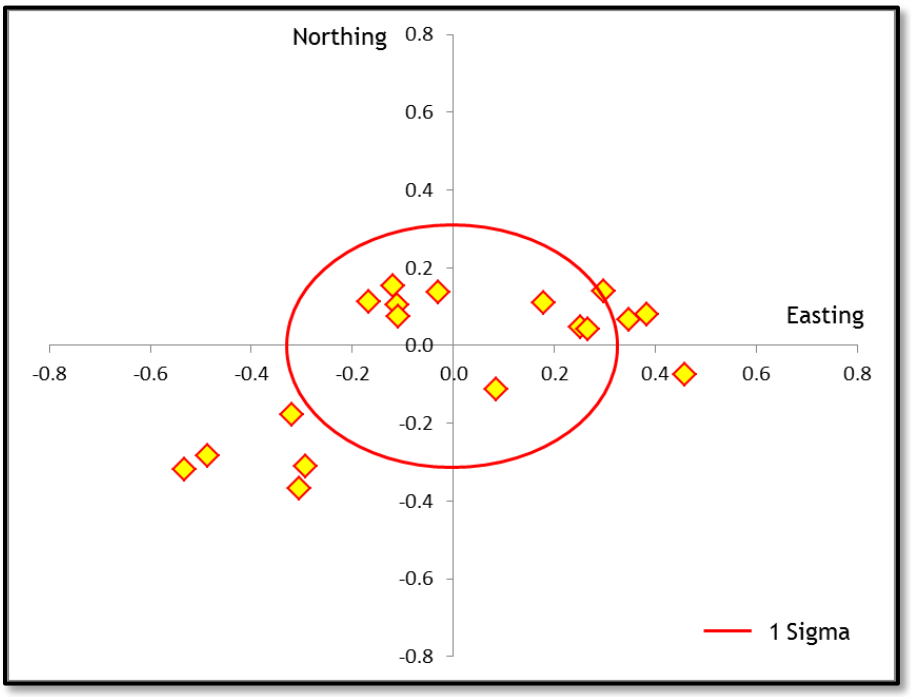


***Figure 15**. Accuracy residuals from comparing RTK of air targets with locations on final thermal mosaics for the Baker Pass study area (units representing accuracy on both axes are in meters)*

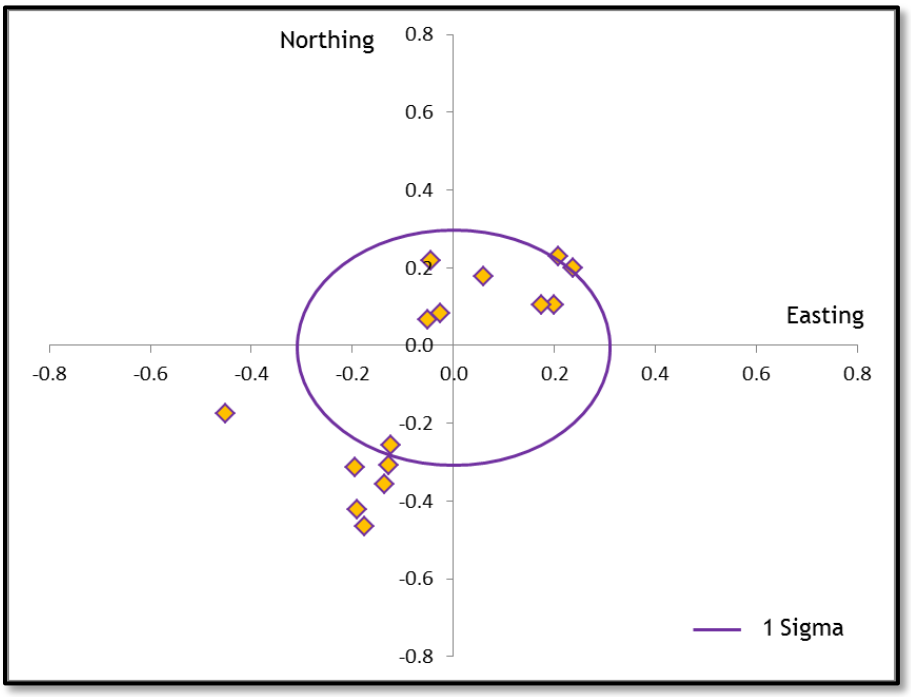

### *2.4.2 Thermal Accuracy Assessment*

The radiant temperatures from the TIR images were compared to the kinetic temperatures measured using the data loggers deployed during the flight over two of the 5 project areas (Table 5). For two locations (SN 2386978 and SN 9951845), radiant temperatures were ~1.2°C warmer than the kinetic temperatures. However, radiant temperatures were warmer for all other locations ranging in difference from 0.9°C to 4.0°C. Review of the imagery indicated that the two locations with warmer radiant temperatures were located in open water and presumably were the most reliable measurements. The remaining data loggers were located in smaller sources of water similar to the location illustrated in Figure 16. The cooler radiant temperatures at these locations and the variability in differences at the smaller sites were expected due to the probability of hybrid or mixed pixels. Consequently, interpretation of the TIR imagery should consider that the actual temperatures of detected geothermal sources are probably greater than represented in the TIR imagery.

***Table 5**. Comparison of recorded temperatures measured at the time of the over flight compared to computed radiant temperatures*

| Sensor | Area | Date | UTC | Local | Kinetic | Radiant | Difference |
|---|---|---|---|---|---|---|---|
| 2386978 | Summer Lake | 3_4_12 | 13:29:10 | 5:29:10 | 10.7 | 12.0 | -1.3 |
| 1026267 | Summer Lake | 3_4_12 | 13:04:23 | 5:04:23 | 3.1 | 1.1 | 2.0 |
| 9951845 | Summer Lake | 3_4_12 | 12:46:41 | 4:46:41 | 10.4 | 11.6 | -1.2 |
| 9951841 | Summer Lake | 3_4_12 | 11:09:41 | 3:09:41 | 13.7 | 9.7 | 4.0 |
| 9951842 | Summer Lake | 3_4_12 | 10:45:44 | 2:45:44 | 12.4 | 11.5 | 0.9 |
| 9911293 | Summer Lake | 3_4_12 | 10:26:42 | 2:26:42 | 5.5 | 2.0 | 3.5 |
| 9951842 | Paulina Marsh | 3_8_12 | 13:31:09 | 5:31:09 | 1.7 | 1.6 | 0.1 |
| 1026267 | Paulina Marsh | 3_9_12 | 9:38:35 | 1:38:35 | 5.7 | 5.8 | -0.1 |

*Christmas Valley, Oregon Military, and Baker Pass AOI's did not have obvious publicly accessible open water to deploy sensors.*

***Figure 16**. The TIR images on the left side of the image show the thermal spatial variability around the logger location. The image in the upper right shows a ground level photo of the same location. The ground level photo illustrates that most pixels at this location will have mixed pixels and hence lower radiant temperatures*

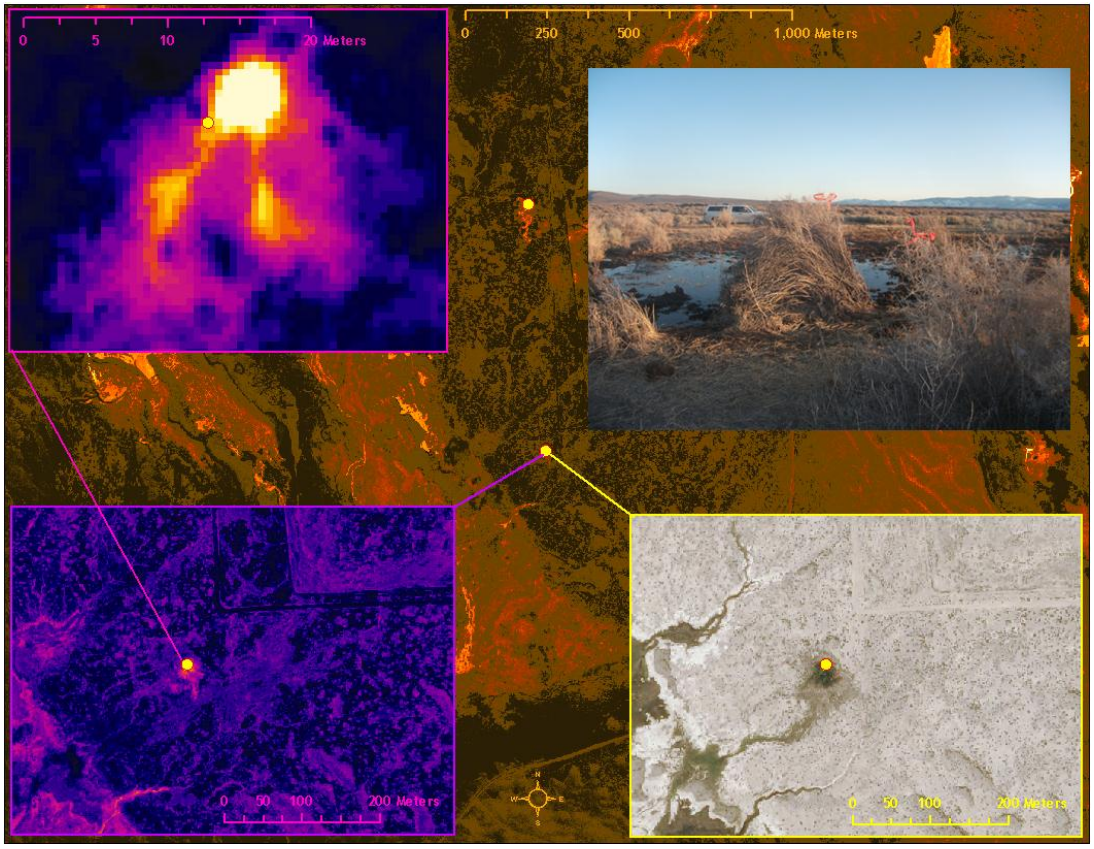


The radiant temperatures for each ground truth location were compared in adjacent flight lines to evaluate any thermal drift in the sensor or acquisition conditions. This comparison resulted in differences of <0.2°C, which was well within the expected range for the sensor. WSI also visually assessed individual flight lines across the study area and observed very little change with flight lines not directly discernible in the thermal mosaic.

## 3. Light Detection and Ranging (LiDAR)

The LiDAR survey utilized a Leica ALS60 sensor mounted in a Cessna Caravan.The Leica system was set to acquire 88,000 laser pulses per second (i.e., 88 kHz pulse rate) and was flown at 1,100 meters above ground level (AGL), capturing a scan angle of ±15° from nadir. With these flight parameters, the laser swath width was 598m and the laser pulse footprint was 26cm. These settings were developed to yield points with an average native pulse density of ≥4 pulses per square meter over terrestrial surfaces. It is not uncommon for some types of surfaces (e.g. dense vegetation or water) to return fewer pulses than the laser originally

emitted. These discrepancies between 'native' and 'delivered' density will vary depending on terrain, land cover, and the prevalence of water bodies.

All areas were surveyed with an opposing flight line side-lap of ≥50% (≥100% overlap) to reduce laser shadowing and increase surface laser painting. The Leica laser systems allowup to four range measurements (returns) per pulse, and all discernible laser returns were processed for the output dataset.

To accurately solve for laser point position (geographic coordinates x, y, z), the positional coordinates of the airborne sensor and the attitude of the aircraft were recorded continuously throughout the LiDAR data collection mission. Aircraft position was measured twice per second (2 Hz) by an onboard differential GPS unit. Aircraft attitude was measured 200 times per second (200 Hz) as pitch, roll and yaw (heading) from an onboard inertial measurement unit (IMU). To allow for post-processing correction and calibration, aircraft/sensor position and attitude data are indexed by GPS time.

## 3.1 Ground Survey – Instrumentation and Methods

During the TIR and LiDAR surveys, static (1 Hz recording frequency) ground surveys were conducted over set monuments. Monument coordinates are provided in Table 2 for each of the Delivery 2 study areas. After the airborne survey, the static GPS data are processed using triangulation with Continuously Operating Reference Stations (CORS) and checked using the Online Positioning User Service (OPUS[1]) to quantify daily variance. Multiple sessions were processed over the same monument to confirm antenna height measurements and reported position accuracy.

Indexed by time, these GPS data are used to correct the continuous onboard measurements of aircraft position recorded throughout the mission. Control monuments were located within 13 nautical miles of the surveyed area.

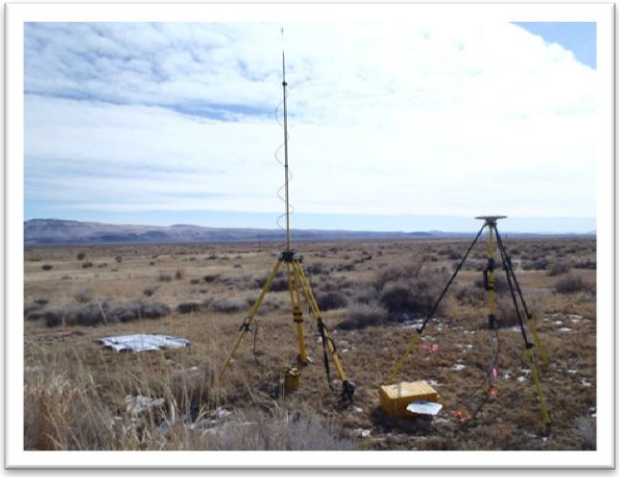

***Figure 17****. Trimble GPS equipment set up for an RTK collection session in the study area*

### *3.1.1 Methodology*

The aircraft was assigned a ground crew member with two Trimble R7 receivers (OPUS ID: TRM 57971.00) and an R8 GNSS receiver (OPUS ID: TRM_R8_GNSS). All control monuments used for aerial acquisition were observed for a minimum of one survey session lasting no fewer than 4 hours and a second session lasting no fewer than 2 hours. At the beginning of every session the tripod and antenna were reset, resulting in two independent instrument

[1] Online Positioning User Service (OPUS) is run by the National Geodetic Survey to process corrected monument positions.

heights and data files. Data was collected at a rate of 1Hz using a 10 degree mask on the antenna.

Aircraft mounted GPS measurements were made during periods with PDOP[2] less than or equal to 3.0 and with at least 6 satellites in view of a stationary reference receiver. Static GPS data collected in a continuous session average the high PDOP into the final solution in the method used by CORS stations. RTK positions were collected on bare earth locations such as paved, gravel or stable dirt roads, and other locations where the ground is clearly visible (and is likely to remain visible) from the sky during the data acquisition and RTK measurement period(s). RTK measurements are not taken on highly reflective surfaces such as center line stripes or lane markings on roads. RTK points were taken no closer than one meter to any nearby terrain breaks such as road edges or drop offs.

The ground crew uploaded the GPS data to our ftp site for QA/QC review and processing in the WSI office. OPUS processing triangulates the monument position using 3 CORS stations resulting in a fully adjusted position. After all data have been collected at each monument, accuracy and error ellipses are calculated from the OPUS reports. This information leads to a rating of the monument based on FGDC-STD-007.2-1998[3] Part 2 Table 2.1 at the 95% confidence level (St Dev $_{NE}$: 0.050 m, St Dev $_{z}$: 0.020 m). When a statistically stable position is found CORPSCON[4] 6.0.1 software is used to convert the UTM positions to geodetic positions. This geodetic position is used for processing the LiDAR data.

## 3.2 Data Processing

### *3.2.1 Applications and Work Flow Overview*

1. Resolved kinematic corrections for aircraft position data using kinematic aircraft GPS and static ground GPS data.

   **Software:** Waypoint GPS v.8.10, Trimble Business Center 2.6
2. Developed a smoothed best estimate of trajectory (SBET) file that blends post-processed aircraft position with attitude data. Sensor head position and attitude were calculated throughout the survey. The SBET data were used extensively for laser point and thermal image processing.

   **Software:** IPAS TC v.3.1
3. Calculated laser point position by associating SBET position to each laser point return time, scan angle, intensity, etc. Created raw laser point cloud data for the entire survey in *.las (ASPRS v. 1.2) format. Data were then converted to orthometric elevations (NAVD88) by applying a Geoid03 correction.

   **Software:** ALS Post Processing Software v.2.74
4. Imported raw laser points into manageable blocks (less than 500 MB) to perform manual relative accuracy calibration and filter for pits/birds. Ground points were then classified for individual flight lines (to be used for relative accuracy testing and calibration).

   **Software:** TerraScan v.12.004

[2]PDOP: Point Dilution of Precision is a measure of satellite geometry, the smaller the number the better the geometry between the point and the satellites.
[3] Federal Geographic Data Committee Draft Geospatial Positioning Accuracy Standards
[4] U.S. Army Corps of Engineers , Engineer Research and Development Center Topographic Engineering Center software

5. Using ground classified points per each flight line, the relative accuracy was tested. Automated line-to-line calibrations were then performed for system attitude parameters (pitch, roll, heading), mirror flex (scale) and GPS/IMU drift. Calibrations were performed on ground classified points from paired flight lines. Every flight line was used for relative accuracy calibration.

   **Software:** TerraMatch v.12.001

6. Position and attitude data were imported. Resulting data were classified as ground and non-ground points. Statistical absolute accuracy was assessed via direct comparisons of ground classified points.

   **Software:** TerraScan v.12.004, TerraModeler v.12.002

7. Bare Earth models were created as a triangulated surface and exported as ArcInfo ASCII grids at a 1 meter pixel resolution. Highest Hit models were created for any class at 1 meter grid spacing and exported as ArcInfo ASCII grids.

   **Software:** TerraScan v.12.004, TerraModeler v.12.002, ARCGIS10

### *3.2.2 Aircraft Kinematic GPS and IMU Data*

LiDAR survey datasets were referenced to the 1 Hz static ground GPS data collected over pre-surveyed monuments with known coordinates. While surveying, the aircraft collected 2 Hz kinematic GPS data, and the onboard inertial measurement unit (IMU) collected 200 Hz aircraft attitude data. Waypoint GPS v.8.10 was used to process the kinematic corrections for the aircraft. The static and kinematic GPS data were then post-processed after the survey to obtain an accurate GPS solution and aircraft positions. IPAS TC v.3.1 was used to develop a trajectory file that includes corrected aircraft position and attitude information. The trajectory data for the entire flight survey session were incorporated into a final smoothed best estimated trajectory (SBET) file that contains accurate and continuous aircraft positions and attitudes.

### *3.2.3 Laser Point Processing*

Laser point coordinates were computed using the IPAS and ALS Post Processor software suitesbased on independent data from the LiDAR system (pulse time, scan angle), and aircraft trajectory data (SBET). Laser point returns (first through fourth) were assigned an associated (x, y, z) coordinate along with unique intensity values (0-255). The data were output into large LAS v. 1.2 files with each point maintaining the corresponding scan angle, return number (echo), intensity, and x, y, z (easting, northing, and elevation) information.

These initial laser point files were too large for subsequent processing. To facilitate laser point processing, bins (polygons) were created to divide the dataset into manageable sizes (<500 MB). Flightlines and LiDAR data were then reviewed to ensure complete coverage of the survey area and positional accuracy of the laser points.

Laser point data were imported into processing bins in TerraScan, and manual calibration was performed to assess the system offsets for pitch, roll, heading and scale (mirror flex). Using a geometric relationship developed by Watershed Sciences, each of these offsets was resolved and corrected if necessary.

LiDAR points were then filtered for noise, pits (artificial low points), and birds (true birds as well as erroneously high points) by screening for absolute elevation limits, isolated points and height above ground. Each bin was then manually inspected for remaining pits and birds and spurious points were removed. In a bin containing approximately 7.5-9.0 million points, an average of 50-100 points are typically found to be artificially low or high. Common sources of non-terrestrial returns are clouds, birds, vapor, haze, decks, brush piles, etc.

Internal calibration was refined using TerraMatch. Points from overlapping lines were tested for internal consistency and final adjustments were made for system misalignments (i.e., pitch, roll, heading offsets and scale). Automated sensor attitude and scale corrections yielded 3-5 cm improvements in the relative accuracy. Once system misalignments were corrected, vertical GPS drift was then resolved and removed per flight line, yielding a slight improvement (<1 cm) in relative accuracy.

The TerraScan software suite is designed specifically for classifying near-ground points (Soininen, 2004). The processing sequence began by 'removing' all points that were not 'near' the earth based on geometric constraints used to evaluate multi-return points. The resulting bare earth (ground) model was visually inspected and additional ground point modeling was performed in site-specific areas to improve ground detail. This manual editing of ground often occurs in areas with known ground modeling deficiencies, such as: bedrock outcrops, cliffs, deeply incised stream banks, and dense vegetation. In some cases, automated ground point classification erroneously included known vegetation (i.e., understory, low/dense shrubs, etc.). These points were manually reclassified.

## 3.3 LiDAR Accuracy Assessment

### *3.3.1 Absolute Accuracy*

Laser point absolute accuracy is largely a function of laser noise and relative accuracy. To minimize these contributions to absolute error, a number of noise filtering and calibration procedures were performed prior to evaluating absolute accuracy. The LiDAR quality assurance process uses the data from the real-time kinematic (RTK) ground survey conducted in the AOI. A total of **397**, **403**, **440**, and **459** RTK GPS measurements were collected for the Christmas Valley, OR Military, Paulina Marsh, and Baker Pass AOI's respectively (Figures 18 – 21). All measurements were collected on hard surfaces and distributed among multiple flight swaths. To assess absolute accuracy the location coordinates of these known RTK ground points were compared to those calculated for the closest ground-classified laser points.

The vertical accuracy of the LiDAR data is described as the mean and standard deviation (sigma ~ $\sigma$) of divergence of LiDAR point coordinates from RTK ground survey point coordinates. To provide a sense of the model predictive power of the dataset, the root mean square error (RMSE) for vertical accuracy is also provided. These statistics assume the error distributions for x, y, and z are normally distributed, thus the skew and kurtosis of distributions are considered when evaluating error statistics.

Statements of statistical accuracy apply to fixed terrestrial surfaces only and may not be applied to areas of dense vegetation or steep terrain.

***Figure 18**. Survey control monuments and RTK checkpoint locations used in the Christmas Valley study area*

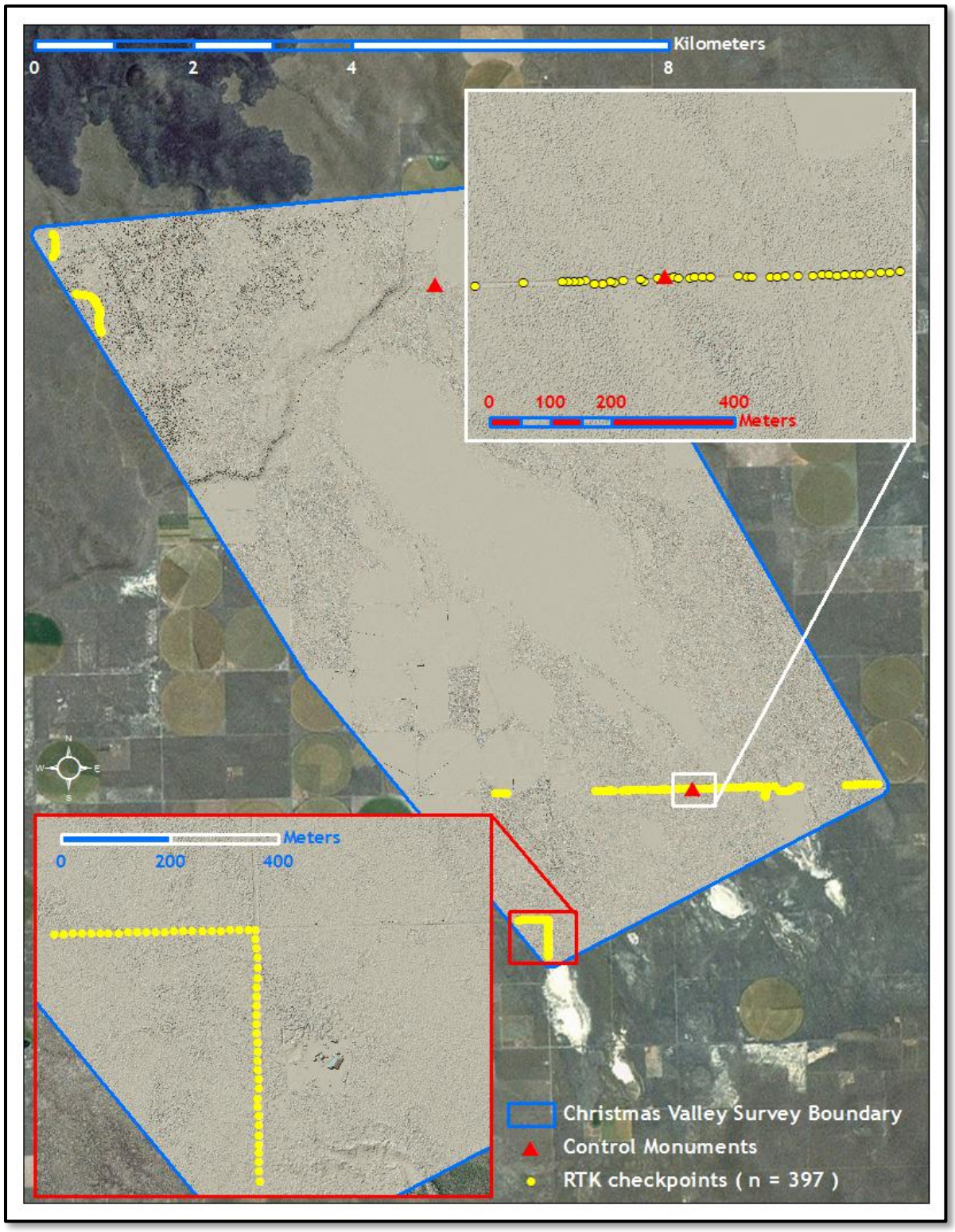

***Figure 19**. Survey control monuments and RTK checkpoint locations used in the Oregon Military study area*

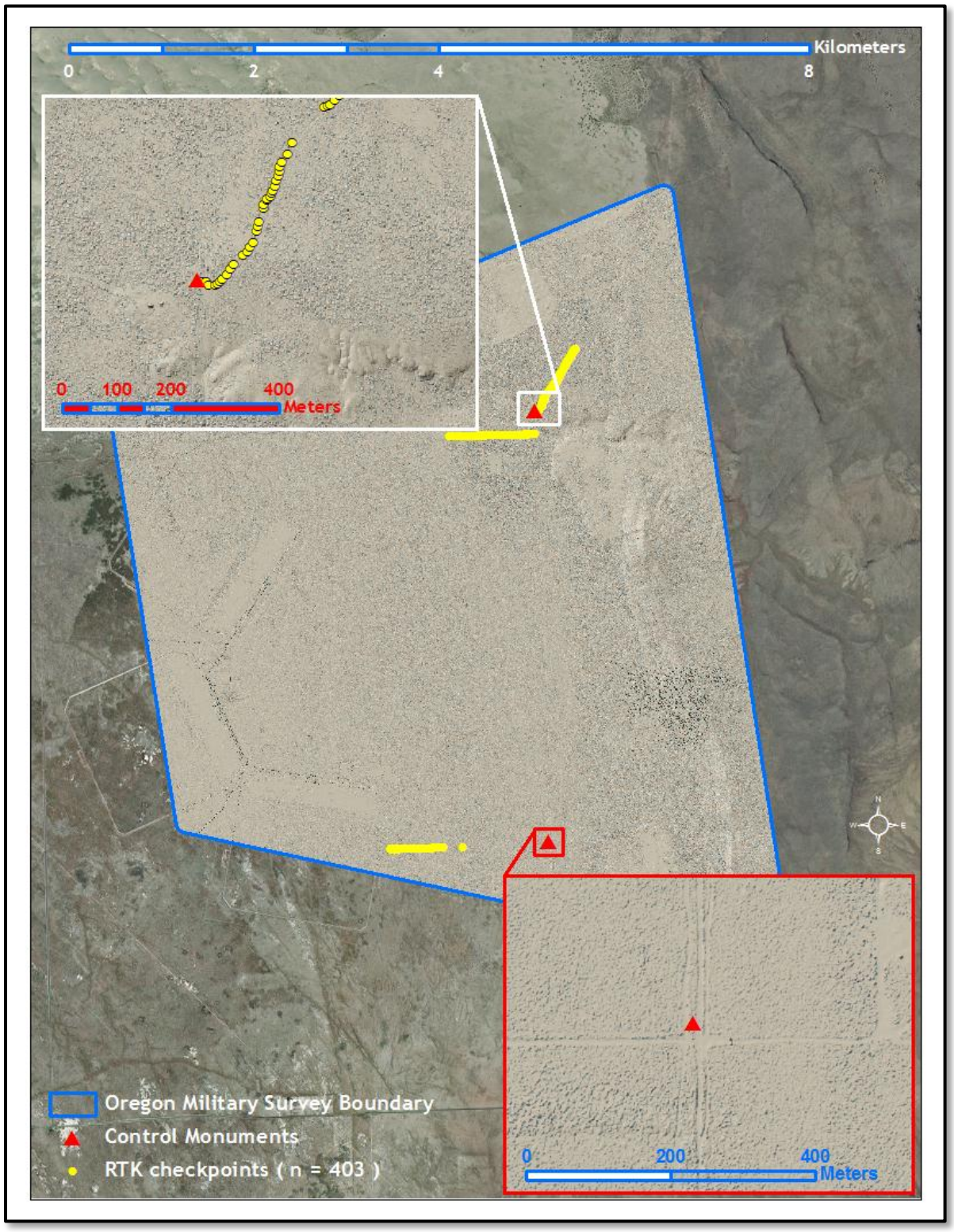

***Figure 20**. Survey control monuments and RTK checkpoint locations used in the Paulina Marsh study area*

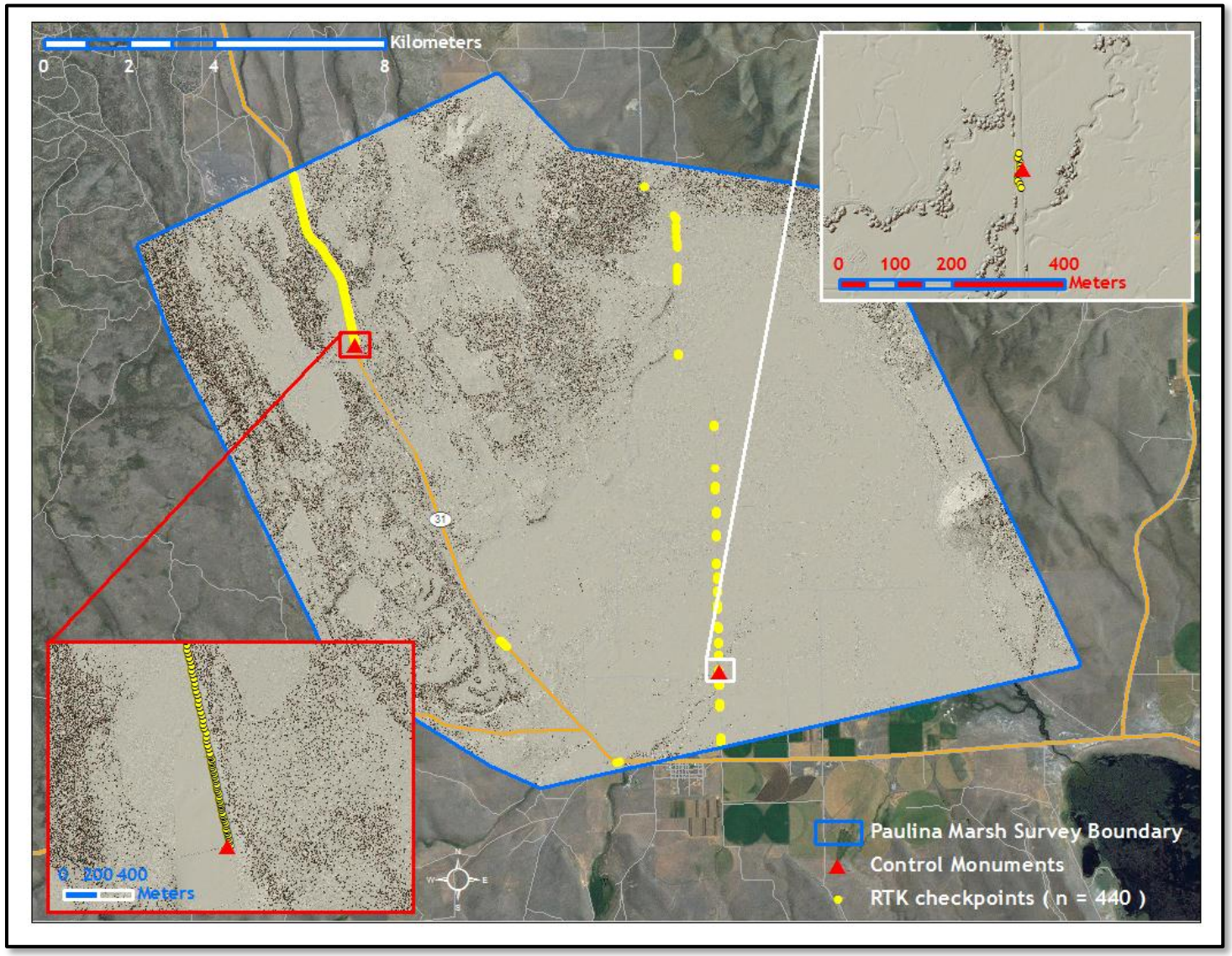

***Figure 21**. Survey control monument and RTK checkpoint locations used in the Christmas Valley study area*

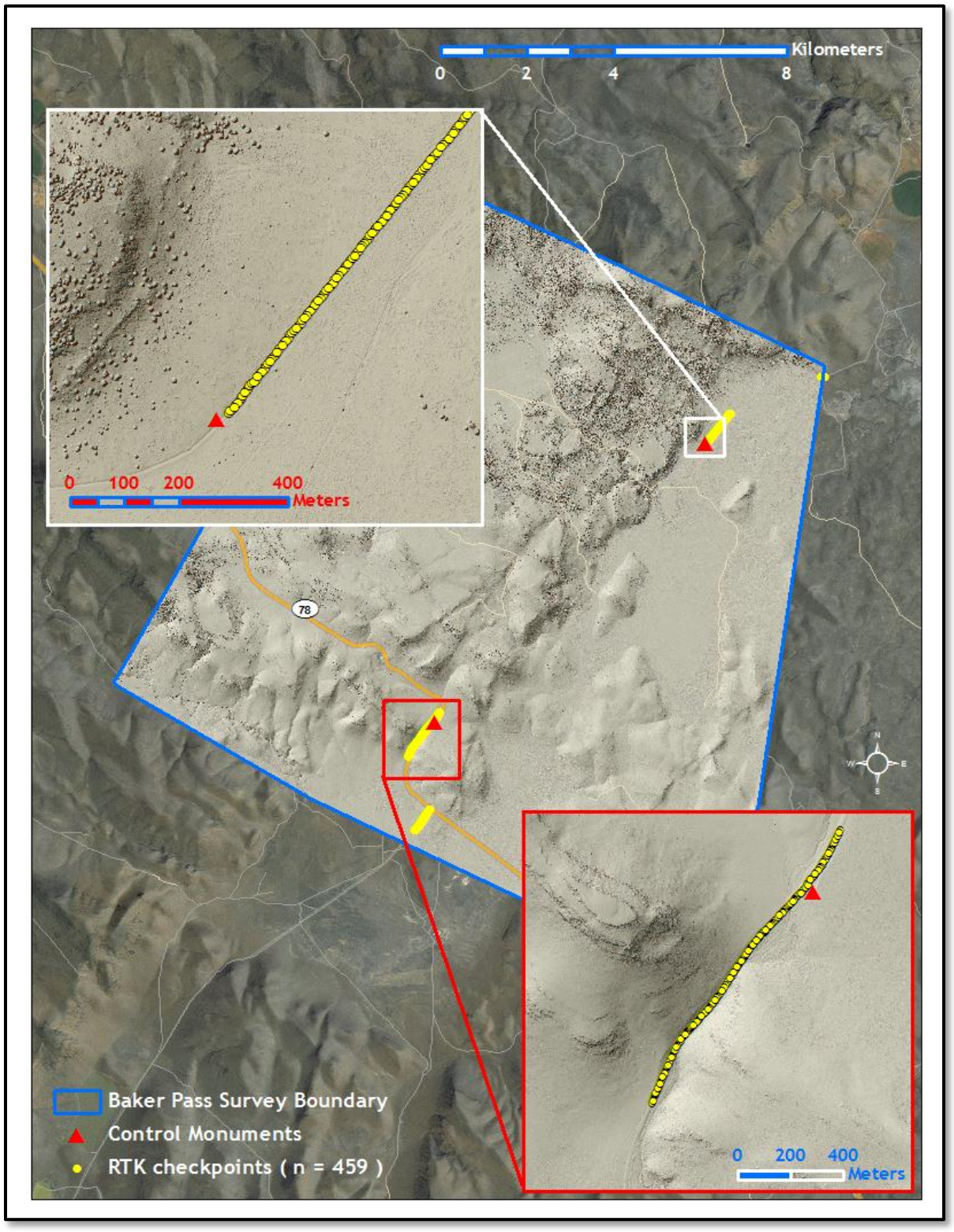

### *3.3.2 LiDAR Data Summary*

Summary statistics for point resolution and accuracy (relative and absolute) of the LiDAR data collected in the Delivery 2 study areas are presented below in terms of central tendency, variation around the mean, and the spatial distribution of the data. The initial LiDAR dataset, acquired to be ≥4 points per square meter was filtered as described previously to remove spurious or inaccurate points. Additionally, some types of surfaces (i.e., dense vegetation, breaks in terrain, water, steep slopes, and highly reflective rock surfaces) may return fewer pulses (delivered density) than the laser originally emitted (native density).

Ground classifications were derived from automated ground surface modeling and manual, supervised classifications where it was determined that the automated model had failed. Ground return densities will be lower in areas of dense vegetation, water, or buildings.

***Table 6***. *Resolution and Accuracy - Specifications and Achieved Values per AOI*

**Christmas Valley**

| | **Targeted** | **Achieved** |
|---|---|---|
| **Resolution:** | ≥ 4 points/$m^2$ | 6.90 points/$m^2$ |
| **Vertical Accuracy (1 σ):** | <15 cm | 2.52 cm |

**OR Military**

| | **Targeted** | **Achieved** |
|---|---|---|
| **Resolution:** | ≥ 4 points/$m^2$ | 6.43 points/$m^2$ |
| **Vertical Accuracy (1 σ):** | <15 cm | 3.54 cm |

**Paulina Marsh**

| | **Targeted** | **Achieved** |
|---|---|---|
| **Resolution:** | ≥ 4 points/$m^2$ | 6.57 points/$m^2$ |
| **Vertical Accuracy (1 σ):** | <15 cm | 3.31 cm |

**Baker Pass**

| | **Targeted** | **Achieved** |
|---|---|---|
| **Resolution:** | ≥ 4 points/$m^2$ | 8.73 points/$m^2$ |
| **Vertical Accuracy (1 σ):** | <15 cm | 2.36 cm |

## LiDAR data resolution per AOI:

**Christmas Valley**
- Average Point (First Return) Density = **6.90 points/m$^2$**
- Average Ground Point Density = **2.57 points/m$^2$**

**OR Military**
- Average Point (First Return) Density = **6.43 points/m$^2$**
- Average Ground Point Density = **2.39 points/m$^2$**

**Paulina Marsh**
- Average Point (First Return) Density = **6.57 points/m$^2$**
- Average Ground Point Density = **2.50 points/m$^2$**

**Baker Pass**
- Average Point (First Return) Density = **8.73 points/m$^2$**
- Average Ground Point Density = **2.71 points/m$^2$**

### *3.3.3 LiDAR Relative Accuracy Calibration Results*

Relative accuracy statistics for each AOI measure the full survey calibration including areas outside the delivered boundary:

**Christmas Valley**
- Project Average = 0.03m
- Median Relative Accuracy = 0.03m
- 1$\sigma$ Relative Accuracy = 0.003m
- 1.96$\sigma$ Relative Accuracy = 0.01m
- RMSE = 0.002m

**OR Military**
- Project Average = 0.03m
- Median Relative Accuracy = 0.03m
- 1$\sigma$ Relative Accuracy = 0.004m
- 1.96$\sigma$ Relative Accuracy = 0.01m
- RMSE = 0.003m

**Paulina Marsh**
- Project Average = 0.03m
- Median Relative Accuracy = 0.03m
- 1$\sigma$ Relative Accuracy = 0.01m
- 1.96$\sigma$ Relative Accuracy = 0.01m
- RMSE = 0.01m

**Baker Pass**
- Project Average = 0.04m
- Median Relative Accuracy = 0.04m
- 1$\sigma$ Relative Accuracy = 0.01m
- 1.96$\sigma$ Relative Accuracy = 0.01m
- RMSE = 0.01m

### *3.3.4 LiDAR Absolute Accuracy*

***Table 7****. Absolute Accuracy – Deviation between laser points and RTK hard surface survey points*

| **Christmas Valley RTK Survey Sample Size (n):**397 | | |
|---|---|---|
| **Root Mean Square Error (RMSE):**0.03m | | **Minimum Δz:-**0.09m |
| **Standard Deviations** | | **Maximum Δz:** 0.07m |
| **1 sigma (σ):** 0.03m | **1.96 sigma (2σ):** 0.05m | **Average Δz:** <0.01m |

| **OR Military RTK Survey Sample Size (n):**403 | | |
|---|---|---|
| **Root Mean Square Error (RMSE):**0.04m | | **Minimum Δz:-**0.09m |
| **Standard Deviations** | | **Maximum Δz:** 0.10m |
| **1 sigma (σ):** 0.04m | **1.96 sigma (2σ):** 0.07m | **Average Δz:** 0.01m |

| **Paulina Marsh RTK Survey Sample Size (n):**440 | | |
|---|---|---|
| **Root Mean Square Error (RMSE):**0.03m | | **Minimum Δz:-**0.09m |
| **Standard Deviations** | | **Maximum Δz:** 0.12m |
| **1 sigma (σ):** 0.03m | **1.96 sigma (2σ):** 0.06m | **Average Δz:** <0.01m |

| **Baker Pass RTK Survey Sample Size (n):**459 | | |
|---|---|---|
| **Root Mean Square Error (RMSE):**0.02m | | **Minimum Δz:-**0.06m |
| **Standard Deviations** | | **Maximum Δz:** 0.09m |
| **1 sigma (σ):** 0.02m | **1.96 sigma (2σ):** 0.05m | **Average Δz:** <0.01m |

# 4. Projection/Datum and Units

| | | |
|---|---|---|
| **Projection:** | | UTM Zone 10N (Christmas Valley, Oregon Military, Paulina Marsh), UTM Zone 11N (Baker Pass) |
| **Datum** | **Vertical:** | NAVD88 Geoid 03 |
| | **Horizontal:** | NAD 83 (CORS96) |
| **Units:** | | Meters |

# 5. Deliverables

## 5.1 TIR Deliverables for each AOI

| | |
|---|---|
| **Raster Data:** | • *TIR mosaic* (GEOtiff format)<br>  ▪ total survey boundary mosaic<br>  ▪ 7.5" quad delineation mosaics<br>• *Rectified Thermal Frames* (GEOtiff format)<br>  ▪ Full Delivery Boundary mosaic<br>  ▪ 0.75" quad delineation<br>• *Unrectified Thermal Frames* (Imagine .img format 640 x 512 pixels) |
| **Vector Data:** | • *Image Frame Index* The actual image frame (or event) locations. The file shows the flight line locations and image times. (shapefile) |
| **Data Report:** | • Full report containing introduction, methodology, and accuracy |

## 5.2 LiDAR Deliverables for each AOI

| | |
|---|---|
| **Point Data:** | • *Ground Classified*(0.75" quad delineation LAS 1.2 format)<br>• *All Returns* (0.75" quad delineation LAS 1.2 format) |
| **Vector Data** | • *0.75" Quad Tile Index* for LiDAR Points (ESRI shapefile format and DGN)<br>• *7.5" Quad DEM Index (*ESRI shapefile format)<br>• *Survey Boundary* (Total Area Flown) (ESRI shapefile format) |
| **Raster Data:** | • *Bare Earth DEM* (7.5" quad delineation 1m ESRI grid format)<br>• *Highest Hit DEM* (7.5" quad delineation 1m ESRI grid format)<br>• *Intensity Images* (0.75" quad delineation 0.5m GEOtiff format) |

# 6. Certifications

Watershed Sciences provided TIR & LiDAR services for the DOGAMI: Christmas Valley, Oregon Military, Paulina Marsh, and Baker Pass study areas as described in this report.

I, Russ Faux, have reviewed the attached report for completeness and hereby state that it is a complete and accurate report of this project.

Russell Faux

Russ Faux
Principal
Watershed Sciences, Inc.

I, Christopher W. Yotter-Brown, being first dully sworn, say that as described in the Ground Survey subsection of the Acquisition section of this report was completed by me or under my direct supervision and was completed using commonly accepted standard practices. Accuracy statistics shown in the Accuracy Section have been reviewed by me to meet National Standard for Spatial Data Accuracy.

Christopher W. Yotter-Brown, PLS Oregon & Washington
Watershed Sciences, Inc
Portland, OR 97204

REGISTERED PROFESSIONAL LAND SURVEYOR
OREGON
JULY 13, 2004
Christopher W. Yotter - Brown
60139 LS
6/18/2012
RENEWAL DATE: 6/30/2012

## 7. Selected Images

***Figure 22****. Image is an aerial view of a spring complex in the northern portion of the Paulina Marsh study area in Lake County, Oregon (Image is a thermal mosaic GEOtiff with a project specific color ramp draped over the LiDAR generated Bare Earth DEM)*

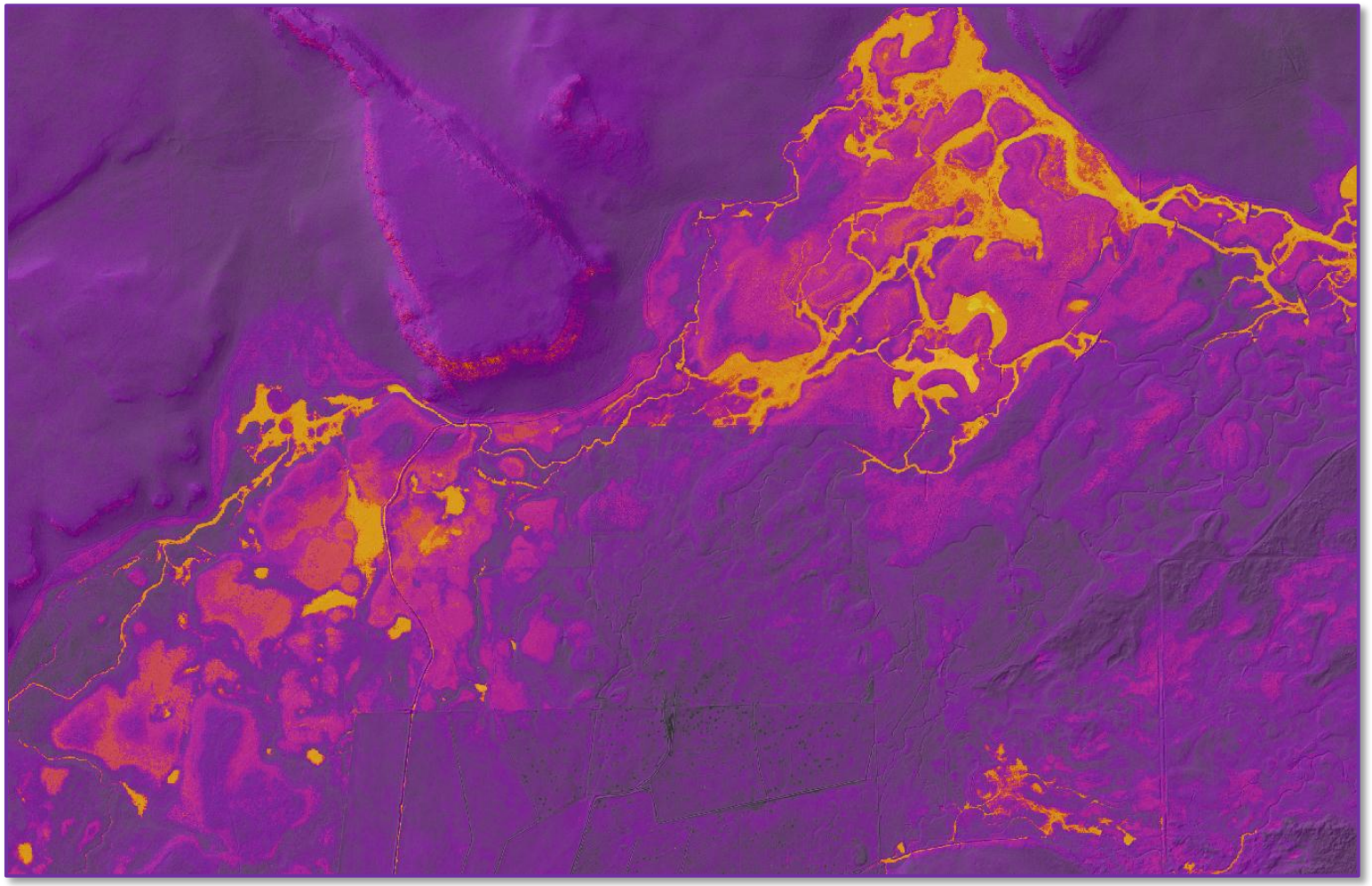

***Figure 23**. Lineaments identified from LiDAR imagery in the Christmas Valley study area (Image is a thermal mosaic GEOtiff with a project specific color ramp to enhance the temperature variation found in the data draped over the LiDAR Bare Earth DEM)*

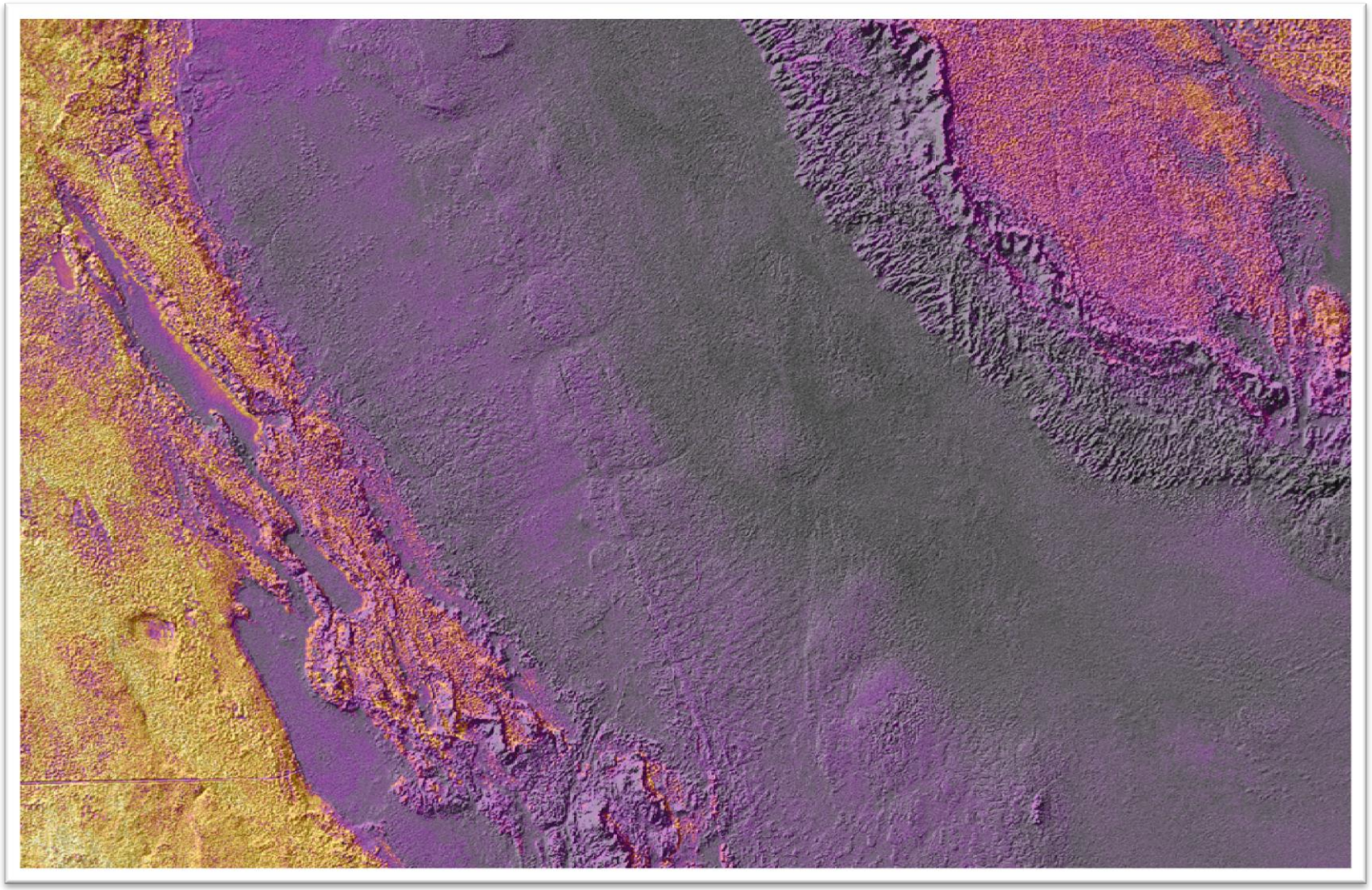

***Figure 24**. Aerial view of a spring and pond complex in the southern portion of Paulina Marsh project area (The image is a thermal mosaic draped over the LiDAR generated Bare Earth hillshade DEM which in concert provide a valuable tool for interpretation of these patters with respect to hyrdology and thermal signature)*

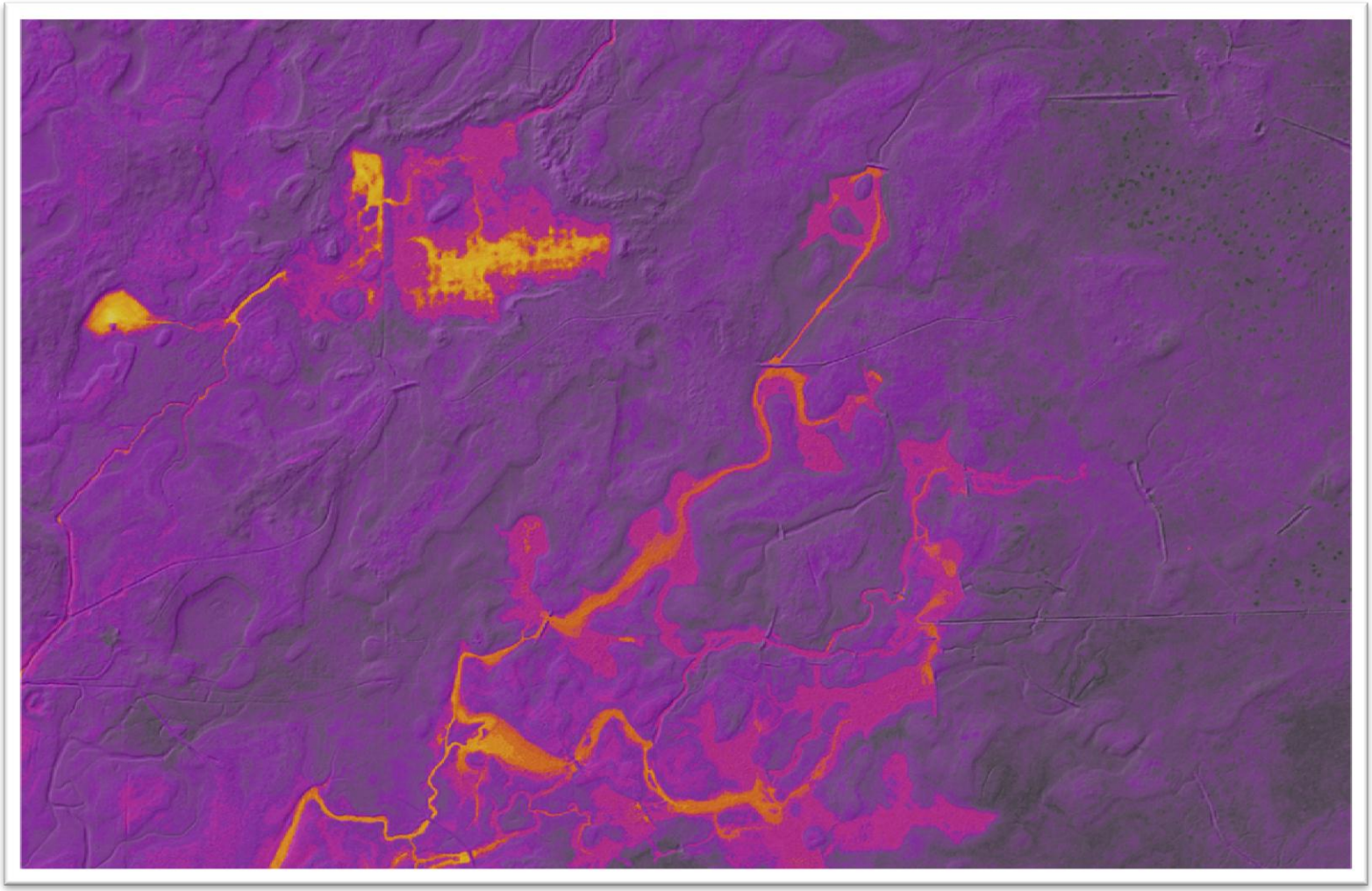

***Figure 25**. Aerial view looking at the northeastern rim of the playa in the Christmas Valley study area, thermal surface expression in this study area was limited to these two ponds (Image is a thermal mosaic draped over the LiDAR generated Highest Hit hillshade DEM)*

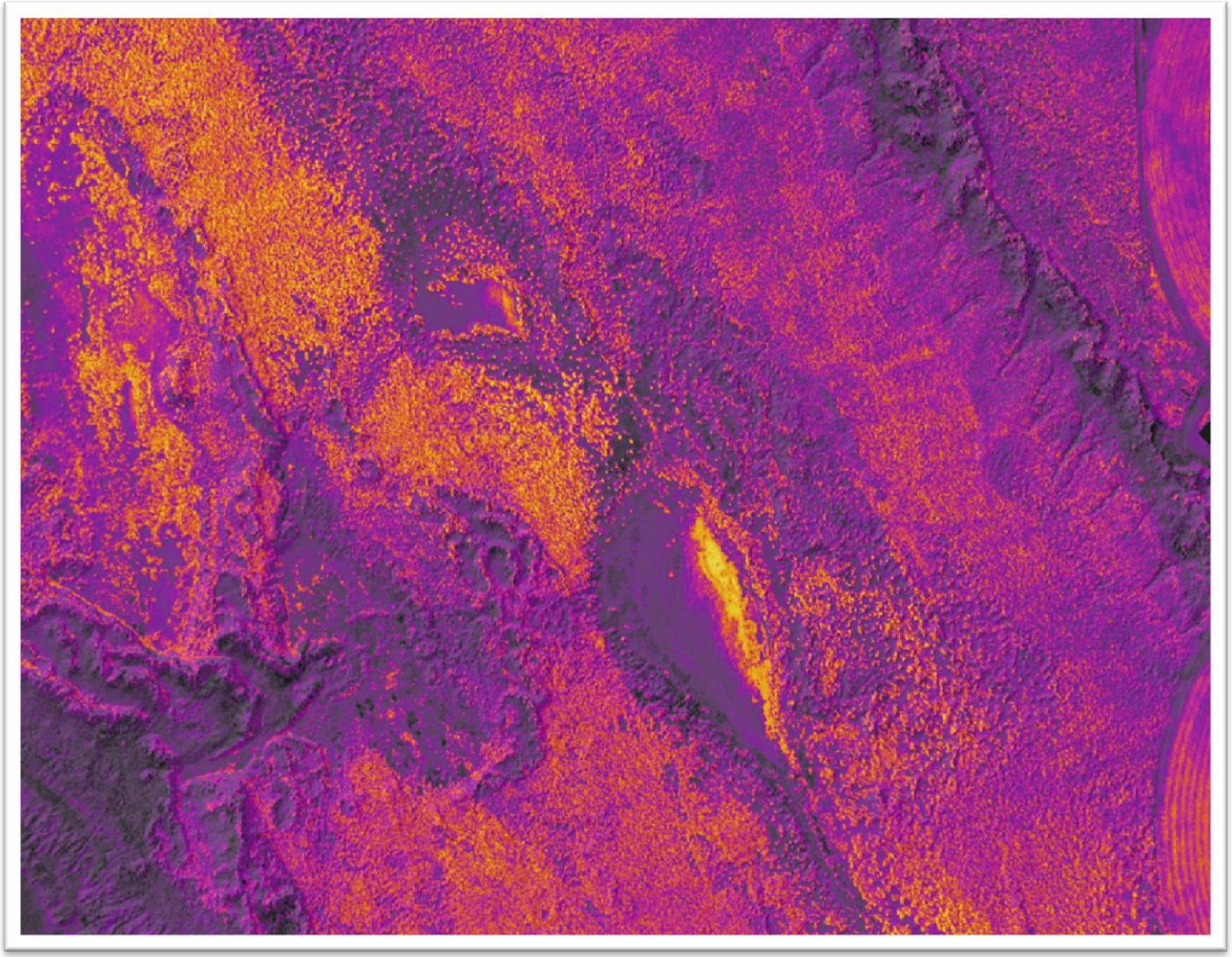

# 8. Glossary

**1-sigma (σ) Absolute Deviation:** Value for which the data are within one standard deviation (approximately 68$^{th}$ percentile) of a normally distributed data set.

**1.96-sigma (σ) Absolute Deviation:** Value for which the data are within two standard deviations (approximately 95$^{th}$ percentile) of a normally distributed data set.

**Root Mean Square Error (RMSE):** A statistic used to approximate the difference between real-world points and the LiDAR points. It is calculated by squaring all the values, then taking the average of the squares and taking the square root of the average.

**Pulse Rate (PR)**: The rate at which laser pulses are emitted from the sensor; typically measured as thousands of pulses per second (kHz).

**Pulse Returns**: For every laser pulse emitted,the Leica ALS 50 Phase II system can record *up to four* wave forms reflected back to the sensor. Portions of the wave form that return earliest are the highest element in multi-tiered surfaces such as vegetation. Portions of the wave form that return last are the lowest element in multi-tiered surfaces.

**Accuracy**: The statistical comparison between known (surveyed) points and laser points. Typically measured as the standard deviation (sigma, σ) and root mean square error (RMSE).

**Intensity Values**: The peak power ratio of the laser return to the emitted laser. It is a function of surface reflectivity.

**Data Density**: A common measure of LiDAR resolution, measured as points per square meter.

**Spot Spacing**: Also a measure of LiDAR resolution, measured as the average distance between laser points.

**Nadir**: A single point or locus of points on the surface of the earth directly below a sensor as it progresses along its flight line.

**Scan Angle**: The angle from nadir to the edge of the scan, measured in degrees. Laser point accuracy typically decreases as scan angles increase.

**Overlap**: The area shared between flight lines, typically measured in percents; 100% overlap is essential to ensure complete coverage and reduce laser shadows.

**DTM / DEM**: These often-interchanged terms refer to models made from laser points. The digital elevation model (DEM) refers to all surfaces, including bare ground and vegetation, while the digital terrain model (DTM) refers only to those points classified as ground.

**Real-Time Kinematic (RTK) Survey**: GPS surveying is conducted with a GPS base station deployed over a known monument with a radio connection to a GPS rover. Both the base station and rover receive differential GPS data and the baseline correction is solved between the two. This type of ground survey is accurate to 1.5 cm or less.

# 9. Citations

Soininen, A., 2004. TerraScan User's Guide. TerraSolid.